

1 **Comparison of AOD, AAOD and column single scattering albedo from AERONET**
2 **retrievals and in-situ profiling measurements**

3 Elisabeth Andrews¹, John A. Ogren², Stefan Kinne³, Bjorn Samset⁴

4 ¹CIRES, University of Colorado, Boulder, CO 80309, USA

5 ²NOAA/ESRL/GMD, Boulder, CO 80305, USA

6 ³Max Planck Institute for Meteorology, 20146 Hamburg, Germany

7 ⁴Center for International Climate and Environmental Research – Oslo (CICERO), 0349 Oslo,
8 Norway

9

10 **Abstract**

11 Here we present new results comparing aerosol optical depth (AOD), aerosol absorption optical
12 depth (AAOD) and column single scattering albedo (SSA) obtained from in-situ vertical profile
13 measurements with AERONET ground-based remote sensing from two rural, continental sites in
14 the US. The profiles are closely matched in time (within +/-3 h) and space (within 15 km) with
15 the AERONET retrievals. We have used Level 1.5 inversion retrievals when there was a valid
16 Level 2 almucantar retrieval in order to be able to compare AAOD and column SSA below
17 AERONET's recommended loading constraint (AOD>0.4 at 440 nm). While there is reasonable
18 agreement for the AOD comparisons, the direct comparisons of in-situ-derived to AERONET-
19 retrieved AAOD (or SSA) reveal that AERONET retrievals yield higher aerosol absorption than
20 obtained from the in-situ profiles for the low aerosol optical depth conditions prevalent at the two
21 study sites. However, it should be noted that the majority of SSA comparisons for AOD₄₄₀>0.2
22 are, nonetheless, within the reported SSA uncertainty bounds. The observation that, relative to
23 in-situ measurements, AERONET inversions exhibit increased absorption potential at low AOD
24 values is generally consistent with other published AERONET/in-situ comparisons across a
25 range of locations, atmospheric conditions and AOD values. This systematic difference in the
26 comparisons suggests a bias in one or both of the methods, but we can not assess whether the
27 AERONET retrievals are biased towards high absorption or the in-situ measurements are
28 biased low. Based on the discrepancy between the AERONET and in-situ values, we conclude
29 that scaling modelled black carbon concentrations upwards to match AERONET retrievals of
30 AAOD should be approached with caution as it may lead to aerosol absorption overestimates in
31 regions of low AOD. Both AERONET retrievals and in-situ measurements suggest there is a
32 systematic relationship between SSA and aerosol amount (AOD or aerosol light scattering) –
33 specifically that SSA decreases at lower aerosol loading. This implies that the fairly common
34 assumption that AERONET SSA values retrieved at high AOD conditions can be used to obtain
35 AAOD at low AOD conditions may not be valid.

36

37 **1. Introduction**

38 The amount and location of absorbing aerosol in the atmosphere is critical for understanding
39 climate change (e.g., Hansen et al., 1997; Ramanathan and Carmichael, 2008; Bond et al.,
40 2013; Samset et al., 2013). Ramanathan and Carmichael (2008) note the effects of absorbing
41 aerosol (which they termed black carbon (BC)) on atmospheric heating rates, precipitation and

42 weather patterns. (Note: The terminology used to refer to absorbing aerosol is imprecise
43 (Petzold et al., 2013, Andreae and Gelencsér, 2006) and encompasses the terms describing
44 chemistry, e.g., 'black carbon' (BC) and terms describing optical effects, e.g., absorption. The
45 measurements reported herein all refer to light absorption.) The vertical distribution of BC can
46 also influence its effect on climate (e.g., Haywood and Ramaswamy, 1998; Samset et al., 2013;
47 Ramanathan and Carmichael, 2008). Single scattering albedo (SSA) is an indicator of the
48 absorbing nature of the aerosol; higher SSA values indicate a more reflective (whiter) aerosol
49 while a more absorbing aerosol will have lower SSA values. SSA is a primary determinant of
50 whether the aerosol will have a warming or cooling effect (e.g., Haywood and Shine, 1995;
51 Hansen et al., 1997; Reid et al., 1998). Uncertainty in the value of SSA due to uncertainties in
52 the amount of absorbing aerosol can even prevent determination of the sign of aerosol forcing
53 on local to regional scales. Bond et al. (2013) assessed BC as the second most important
54 global-average warming species (top-of-atmosphere forcing $+1.1 \text{ W m}^{-2}$, 90% bounds: $+0.17$ to
55 $+2.1 \text{ W m}^{-2}$) after CO_2 (in Bond et al. (2013) the direct effect of BC is 0.71 , 90% bounds: $+0.09$
56 to 1.26 W m^{-2}).

57
58 Currently, the only way vertical profiles of aerosol absorption can be obtained is via airborne in-
59 situ measurements. Such flights are expensive and tend to primarily occur during intensive
60 field campaigns, which are usually aimed at studying specific aerosol types (e.g., biomass
61 burning, African dust, urban/industrial pollution). This reliance on short-term campaigns results
62 in profile data sets that are sporadic in both space and time, and not necessarily representative
63 of typical conditions. Additional issues with airborne in-situ measurements include adjustment
64 of measurements to ambient conditions, particle losses in sample lines, and instrument
65 uncertainties. Nonetheless, in-situ vertical profiling of absorbing aerosols has provided useful
66 information to modelers trying to understand climate effects, transport, and lifetimes of these
67 important atmospheric constituents (e.g., Koch et al., 2009; Schwarz et al., 2010; Skeie et al.,
68 2011).

69
70 The limited availability of in-situ vertical profile measurements means modelers must rely on
71 globally sparse and/or temporally sporadic airborne measurements to evaluate BC vertical
72 distributions in their models. Alternatively, the column properties retrieved from AERONET
73 measurements and inversions have been widely used to provide a first constraint on modeled
74 vertical aerosol properties (e.g., Sato et al., 2003; Koch et al., 2009; Bond et al., 2013; He et al.,
75 2014; Wang et al., 2014). Use of the AERONET data as an absorption constraint has
76 suggested upscaling of modeled AAOD values by a factor of 2-6 depending on location (e.g.,
77 Bond et al., 2013), although Wang et al. (2016) has shown that better spatial resolution of
78 models and emission inventories can reduce some of the previously observed model/AERONET
79 discrepancies.

80
81 Ground-based remote sensing of both direct attenuation and sky radiances permit inversions of
82 atmospheric column averaged absorption. By retrieving the complex refractive indices at
83 different solar wavelengths as well as the average aerosol size-distribution, absorption related
84 properties can be determined (e.g., aerosol absorption optical depth (AAOD), single scattering
85 albedo (SSA) and, absorption Ångström exponent (AAE)). The AERONET network has a fairly

86 wide spatial coverage on land, with long data records at many sites (Holben et al., 1998;
87 Dubovik et al., 2000; Dubovik and King, 2000). One obvious limitation of the AERONET
88 inversion retrievals is that the uncertainty of the derived single scattering albedo (SSA) becomes
89 very large at low values of AOD (Dubovik et al., 2000). To minimize the effects of this
90 uncertainty, the AERONET Level-2 data invalidates all absorption-related values if the AOD at
91 wavelength 440 nm (AOD_{440}) is below 0.4 (Dubovik et al., 2000; Dubovik et al., 2002; Holben et
92 al., 2006). Unfortunately, this restriction greatly reduces the spatial and temporal coverage of
93 absorption-related data that can be obtained from AERONET. Moreover, by excluding low AOD
94 cases, the climatological statistics of AAOD derived from the AERONET Level-2 data may be
95 biased high.

96
97 Model analysis of global AOD values suggest that 95% of global AOD_{440} values are below 0.4
98 (Figure 1), while 89% of the AOD_{440} values over land are below the 0.4 threshold. Five models
99 in the AeroCom suite (GMI-MERRA-v3, GOCART-v4, LMDZ-INCA, OsloCTM2, and
100 SPRINTARS-v385) have reported daily-average values of AOD_{440} (for AeroCom Phase II
101 control experiment), which can be used to develop a cumulative frequency distribution of the
102 percent of the Earth's surface and days where a Level-2 AERONET retrieval of AAOD might be
103 possible (ignoring the presence of clouds and absence of sunlight). Figure 1 indicates that, at
104 best, Level-2 AERONET AAOD retrievals might represent 5% of the days, globally, and less
105 than 11% of the days over land. In other words, the AOD constraint on Level-2 AERONET
106 almucantar inversion retrievals means these retrievals represent only a small fraction of the
107 Earth's surface and are biased to conditions of high aerosol loading.

108
109 The other information that Figure 1 provides is the fractional contribution of regions with different
110 AOD_{440} amounts to the total aerosol and the fossil fuel black carbon (BCFF) radiative budget.
111 These values were derived from monthly data from 4 models in the AeroCom suite. The
112 fractional contribution to the radiative budget can be mathematically described as follows: for
113 each model grid box there are three quantities: (i) the radiative forcing ($W m^{-2}$), (ii) the horizontal
114 area of the box (m^2), and (iii) the AOD_{440} . The product of the radiative forcing term and area is
115 the perturbation to Earth's radiative budget due to total aerosol (or BCFF) in the box. The sum
116 of this product over all the boxes is the total perturbation. Figure 1 shows the fraction of the
117 radiative budget perturbation as a function of AOD_{440} . It suggests that approximately 75% of the
118 total aerosol forcing and 83% of BCFF forcing is due to regions of the globe where $AOD_{440} < 0.4$.
119 This highlights the significant contribution of aerosol in these cleaner areas to the total global
120 radiation budget.

121
122 It should be noted that there is significant inter-model variation in the AeroCom cumulative
123 AOD_{440} and radiative forcing plots shown in Figure 1. In particular the BCFF cumulative forcing
124 fraction varies with the lifetime of BC predicted by the models. A long BC lifetime results in more
125 dilute AOD and BCFF radiative forcing distributions. Other issues include the fact that global
126 models have limited spatial and temporal resolution, and generally simulate less variability in
127 aerosol properties than is observed in measurements. However, all models used to generate
128 Figure 1 follow the same general trend as is shown in Figure 1 with the take-away point being
129 that AOD_{440} values > 0.4 are a relatively rare occurrence.

130
131 Because of the potential of the AERONET absorption-related retrievals (e.g., AAOD and SSA)
132 for understanding global distributions of absorbing aerosol, there have been many studies
133 comparing AERONET retrieval values with those obtained from in-situ measurements in order
134 to assess the AERONET retrieval validity. Such comparisons have taken several different
135 forms. There have been direct comparisons where column SSA or AAOD values calculated
136 from individual in-situ vertical profiles have been compared with AERONET retrieved values for
137 retrievals close in time and space (Haywood et al., 2003; Magi et al., 2005; Mallet et al., 2005;
138 Leahy et al., 2007; Corrigan et al., 2008; Osborne et al., 2008; Johnson et al., 2009; Esteve et
139 al., 2012; Schafer et al., 2014). In addition to direct comparisons there have been general,
140 statistical assessments between AERONET and in-situ measurements for both SSA and AAOD
141 including: (a) comparing surface in-situ measurements with AERONET retrievals (e.g., Dubovik
142 et al., 2002; Doran et al., 2007; Mallet et al., 2008; Corr et al., 2009); (b) comparing in-situ SSA
143 (or AAOD) from a few flight segments to the corresponding column SSA (or AAOD) from
144 AERONET (e.g., Kelecksoglou et al., 2012; Müller et al., 2012) and (c) comparison of statistical
145 distributions or averages of AERONET retrievals for a given time period with airborne in-situ
146 measurements (e.g., Ramanathan et al., 2001; Leahy et al., 2007; Andrews et al., 2011a;
147 Ferrero et al., 2011; Johnson et al., 2011). Many of these statistical comparisons have shown
148 good agreement between the AERONET and in-situ values. This increases general confidence
149 in the AERONET retrievals. However, such statistical comparisons are not appropriate for the
150 evaluation of the accuracy of individual retrievals.

151
152 The primary scientific question to be addressed in this paper is: *Is there a consistent bias*
153 *observed between AAOD and column SSA obtained from in-situ profiling flights and AERONET*
154 *retrievals?* The answer to this question may help determine the validity of adjusting model
155 estimates of AAOD to agree with AERONET retrievals (e.g., Sato et al., 2003; Bond et al.,
156 2013). It should be noted that AERONET does not recommend the use of absorption-related
157 parameters (e.g., single scattering albedo, absorption aerosol optical depth, and complex index
158 of refraction) at AOD₄₄₀ below 0.4. Dubovik et al. (2000) suggests the uncertainty of AERONET
159 SSA values more than doubles for AOD₄₄₀ less than 0.2.

160 In what follows, we first evaluate how direct AERONET AAOD retrievals compare with those
161 derived from multi-year, in-situ measurements obtained from vertical profiles over two rural
162 continental AERONET sites in the U.S. Second, we create a summary of all direct AAOD or
163 SSA comparisons between in-situ vs. AERONET data previously presented in the literature in
164 order to place our results about AERONET aerosol absorption-related retrievals in a wider
165 context. Finally, we look at the seasonality of in-situ, AERONET, and modelled (AeroCom) SSA
166 and AAOD values to see if the annual cycles can provide any insight into observed
167 discrepancies in the direct comparisons. Because this study focuses on only two low AOD sites
168 in the continental US which are unlikely to be generally representative of other low loading sites
169 around the globe, and because other factors (e.g., Wang et al., 2016) may contribute to
170 reported differences between modelled and AERONET AAOD we do not attempt to suggest
171 implications for global BC forcing.

172

173 2. Methods

174 This study utilizes data from two sites with collocated AERONET measurements and multi-year,
175 in-situ aerosol profiling measurements. The two sites are Bondville (BND, 40.05°N 88.37°W,
176 230 m asl) and Southern Great Plains (SGP, 36.61°N 97.49°W, 315 m asl). Surface in-situ
177 measurements and AERONET column measurements have been made at both locations since
178 the mid-1990s (e.g., Delene and Ogren, 2002; Sheridan et al., 2001; Holben et al., 1998).
179 Weekly to twice-weekly flights measuring in-situ vertical profiles of aerosol optical properties
180 over these two sites were made for a subset of the years of ground-based observations. At SGP
181 the in-situ profile flights were centered over the site's central facility where the AERONET
182 sunphotometer is deployed. Due to FAA flight restrictions, the BND in-situ profiling flights took
183 place approximately 15 km to the WNW of the AERONET sunphotometer location at the BND
184 surface site (Sheridan et al., 2012). Additionally, for BND, a low level flight leg (200 m agl) was
185 flown directly over the instrumented BND surface site. The flights at both sites were subject to
186 'visual flight regulations' which means they took place during daylight hours and the plane did
187 not fly in-cloud.

188
189 At BND and SGP, the median AOD₄₄₀ values are 0.14 and 0.11, respectively (based on all
190 AERONET Level-2 data from the start of AERONET measurements at each site). These median
191 values fall right around the 50% mark on the AOD cumulative distribution plot (Figure 1),
192 indicating BND and SGP may be appropriate sites to explore potential discrepancies between
193 AERONET and in-situ AAOD and SSA retrievals at lower AOD conditions.

194
195 2.1 IN-SITU

196 The in-situ aerosol profiles were obtained with dedicated Cessna 206 airplanes flying stair-step
197 profiles one to two times per week over the two sites. Between 2006 and 2009, 365 flights were
198 flown over BND (out of a total of 401 flown in the region (Sheridan et al., 2012)), while 171
199 aerosol profile flights were flown over SGP in the 2005-2007 time period (Andrews et al.,
200 2011a). The profiles consisted of 10 (at BND) or 12 (at SGP) level flight legs between
201 approximately 450 and 4600 m asl (corresponding to approximately 150 and 4200 m agl). The
202 profiles, which were 'stair-step' descents, took approximately 2 hours to complete as the
203 airplane spent set amounts of time at each level (10 min/flight level for flight legs above ~1600
204 m asl and 5 min/flight level for flight legs below that altitude) in order to improve measurement
205 statistics at the typically cleaner higher altitude flight levels. Airplane speed was approximately
206 50 m/s, resulting in the 10 min upper level legs being approximately 30 km long and the 5 min
207 lower level legs approximately half that (15 km) length. This flight pattern means the last 30 min
208 of the profile were typically in the boundary layer for these two sites and encompassed the
209 majority of the aerosol contribution to column aerosol loading. Previous work has shown that
210 the airplane measurements appear to capture the variability in aerosol properties observed by
211 the long-term, continuous measurements at the surface (e.g., Figure 3 in Andrews et al., 2004)

212 Descriptions of the flight profiles and aircraft package have been described in detail in other
213 papers (Andrews et al., 2011a; Sheridan et al., 2012) so only a brief description is provided

214 here. The pilot flew within the constraints provided (specifically-defined staircase profile, vary the
215 time of day, cross wind, over the instrumented field site, during daylight and not within clouds)
216 but without day-to-day scheduling input from scientists. Here, we utilize the same 10 flight levels
217 for both profiling sites: 457, 609, 915, 1219, 1829, 2439, 3050, 3659 and 4575 m asl. Of the
218 365 flights at BND, 253 flights had complete profiles (all flight levels) with valid scattering,
219 absorption and relative humidity data; at SGP, 132 flights out of 171 were complete. Only
220 complete profiles (all 10 flight levels) were used in this analysis. As is obvious from the vertical
221 range of the flight levels, complete in-situ profiles do not equate to complete atmospheric
222 profiles – this is discussed more in the in-situ uncertainties discussion (Section 2.4.1). The
223 number of flights that could be compared with AERONET measurements is significantly less
224 than this, as discussed in Section 2.3 where the merging of the AERONET and in-situ data sets
225 is described.

226
227 The aircraft were equipped with an inlet that sampled particles with aerodynamic diameter $D_p < 7$
228 μm , and losses in downstream sample lines were estimated to reduce the particle diameter for
229 50% sampling efficiency to 5 μm (Sheridan et al., 2012). Aerosol light absorption (σ_{ap}) was
230 measured at three wavelengths (467, 530, 660 nm) using a Radiance Research Particle-Soot
231 Absorption Photometer (PSAP) and aerosol light scattering (σ_{sp}) was measured at three similar
232 wavelengths (450, 550, 700 nm) using an integrating nephelometer (TSI model 3563). The
233 measurements of absorption and scattering were made at low relative humidity (RH<40%).
234 Absorption data were corrected for scattering artifacts, flow and spot size calibrations, etc.,
235 using the Bond et al. (1999) algorithm, with appropriate modifications for wavelength (Ogren,
236 2010). The Anderson and Ogren (1998) correction for instrument non-idealities was applied to
237 the nephelometer data.

238
239 Ambient temperature (T_{amb}) and RH (RH_{amb}) were measured by a sensor (Vaisala Inc, Model
240 Humicap 50Y) mounted on the aircraft fuselage inside a counterflow inlet shroud, and the
241 nephelometer sample pressure was used as a surrogate for ambient pressure. These
242 measurements of ambient meteorological parameters were used to adjust the in-situ optical
243 data to ambient conditions in order to compare with the AERONET measurements and
244 retrievals, which are made at ambient conditions. Climatological IMPROVE network surface
245 aerosol chemistry measurements of sulfate and organic carbon (Malm et al., 1994) were utilized
246 to determine a value for the hygroscopic growth parameter ' γ ' for each site based on the Quinn
247 et al. (2005) parameterization which relates aerosol hygroscopicity to organic mass fraction.
248 For BND $\gamma=0.71\pm 0.08$, while for SGP $\gamma=0.65\pm 0.08$. At BND the IMPROVE chemistry
249 measurements are co-located at the profile location, while for SGP the measurements at the
250 IMPROVE Cherokee Nation site (approximately 56 km southwest of the profile location) were
251 used. This γ value was then used in conjunction with the airborne RH_{amb} measurements to
252 adjust the in-situ scattering profiles for both SGP and BND.

253
254 The equation used to adjust the dry, in-situ scattering to ambient relative humidity (RH_{amb}) is a
255 commonly used aerosol hygroscopic growth parameterization (e.g., Kasten, 1969; Hanel, 1976;
256 Kotchenruther et al., 1999; Carrico et al., 2003; Crumeyrolle et al., 2014):

257

258
$$\sigma_{sp}(RH_{amb})/\sigma_{sp}(RH_{dry})=a*(1-(RH_{amb}/100))^{-\gamma}. \quad (1)$$

259

260 where $\sigma_{sp}(RH_{amb})$ is the aerosol scattering at ambient RH, $\sigma_{sp}(RH_{dry})$ is the measured scattering
261 at low RH, and γ is the hygroscopic growth parameter derived from the IMPROVE aerosol

262 chemistry. The value of 'a' can be determined using: $a = (1/(1-RH_{dry}/100))^{-\gamma}$ (e.g., Crumeyrolle
263 et al., 2014; Quinn et al., 2005). Here we assume $a=0.9$ based on the typical RH values
264 measured inside the nephelometer for both profile locations (BND $RH_{dry}=12\pm 11\%$; SGP
265 $RH_{dry}=14\pm 10\%$). RH_{amb} at BND and SGP averaged 47.4% and 38.6%, respectively, over all
266 flight levels and seasons (56% (BND) and 43% (SGP) below 1500 m asl). The 95th percentile
267 RH_{amb} values (calculated over all flights and flight levels) were 79.3% and 76.6% at BND and
268 SGP, respectively. (Note: scattering-weighted column average RH values were 54% at BND
269 and 43% at SGP). Applying eq. 1 to the observed RH_{amb} and $\sigma_{sp}(RH_{dry})$ profiles, the average
270 enhancement of column-average σ_{sp} due to hygroscopic growth was 1.52 and 1.36 at BND and
271 SGP, respectively. The corresponding 95th percentiles of column average enhancement of
272 scattering were 2.06 and 2.10. While Equation 1 takes into account differences in hygroscopic
273 growth due to RH for each segment of each flight, it does not account for compositional
274 changes that might affect the scattering enhancement due to hygroscopicity. For aerosol
275 events such as biomass burning and dust episodes with significantly different composition than
276 the 'normal' aerosol we would expect to over-predict the aerosol hygroscopicity relative to the
277 normal aerosol. Sheridan et al., (2001) showed that the SGP surface aerosol had lower
278 hygroscopicity when it was influenced by dust or smoke.

279

280 The absorption measurements were adjusted to ambient temperature and pressure, but not to
281 ambient RH because the parameterization of the correction and its magnitude are unknown. It
282 is typically assumed that absorbing aerosol is hydrophobic (e.g., Schmid et al., 2003; Reid et al.,
283 2005; Schaefer et al., 2014), i.e., does not take up water. The uncertainties associated with this
284 assumption are discussed in section 2.4.

285

286 Both the scattering and absorption in-situ measurements were adjusted to the two nominal
287 Level-2 AERONET wavelengths in the mid-visible spectrum (440 nm and 675 nm). The 440 nm
288 wavelength is of interest as that is the wavelength for which the AOD constraint for retrieving
289 SSA and hence, AAOD, is given; the 675 nm wavelength is also presented because it is less
290 sensitive to NO_2 , organics, and dust which could potentially bias the in-situ/AERONET
291 comparison. Also, evaluating data at both wavelengths helps in attributing aerosol absorption to
292 BC versus dust, since at 675 nm absorption is almost entirely caused by BC. The measured
293 scattering Ångström exponent was used to adjust the in-situ scattering measurements to the
294 AERONET wavelengths. For the in-situ aerosol absorption wavelength adjustments we used a
295 constant absorption Ångström exponent of 1.2 to minimize the effects of noise in the
296 measurement. Previous studies have shown that for both BND and SGP the absorption
297 Ångström exponent is ~1.0 in the BL and 1.5 at higher altitudes (Andrews et al., 2011; Sheridan
298 et al., 2012). Using the incorrect absorption Ångström exponent will have a negligible effect on
299 the resulting absorption value because of the small difference between the measured and target

300 wavelengths; using an absorption Ångström exponent of 1.2 instead of 1.0 will result in a 1%
301 difference in adjusted wavelength while using an Ångström exponent of 1.2 instead of 1.5 will
302 result in a 2% difference in adjusted absorption.

303
304 Finally, using these in-situ values adjusted to AERONET wavelengths and ambient conditions
305 the flight profile average properties can be determined. Aerosol extinction ($\sigma_{ep} = \sigma_{sp} + \sigma_{ap}$) was
306 calculated and integrated vertically for the profile to obtain the in-situ AOD. The aerosol
307 absorption for each profile was integrated vertically to obtain the in-situ AAOD. As described in
308 Andrews et al. (2004), the in-situ column SSA (which is compared to the AERONET SSA value
309 in section 3.1) was calculated for each flight level and then extinction-weighted and integrated to
310 determine column SSA. This results in SSA values which are virtually identical to SSA values
311 calculated using: $SSA_{col,in-situ} = (AOD_{in-situ} - AAOD_{in-situ})/AOD_{in-situ}$ and effectively gives higher
312 weighting to the SSA values at altitudes that had the highest aerosol concentrations. Details of
313 the procedure for calculating the vertical integral are given in Andrews et al. (2004), although, in
314 this study, the in-situ profiles contained two additional high altitude flight levels (at 3659 and
315 4575 m asl) and the layer at the highest altitude was assumed to extend 457 m above the
316 measurement altitude. Profile statistics for various parameters including SSA are provided in
317 Andrews et al. (2004, 2011a) and Sheridan et al. (2012). Individual flight profiles for various
318 parameters are available online at: http://www.esrl.noaa.gov/gmd/aero/net/iap/iap_profiles.html
319 (for SGP) and https://www.esrl.noaa.gov/gmd/aero/net/aao/aao_prof2007.html (for BND).

320 2.2 AERONET

321 AERONET measurements have been made at BND since mid-1995 and at SGP since mid-
322 1994. The AERONET network makes spectral measurements of aerosol optical depth (AOD)
323 using CIMEL sun/sky radiometers (Holben et al., 1998). The measurements are typically made
324 at seven wavelengths, with an eighth wavelength used for water vapor measurements. The
325 AERONET website (<http://aeronet.gsfc.nasa.gov>) provides links to data from more than 500
326 sites across the globe. The column extinction Ångström exponent (\AA) can be directly calculated
327 from the wavelength-dependent AOD measurements (Eck et al., 1999). In addition to AOD and
328 \AA , algorithms have been developed utilizing both the spectral AOD and the spectral angular
329 distribution of the sky radiances obtained from almucantar scans, which enable retrieval of other
330 column aerosol properties including AAOD, SSA, size distribution, complex refractive index, and
331 fine mode fraction of extinction (FMF_e) (Dubovik and King, 2000; Dubovik et al., 2000; O'Neill et
332 al., 2003; Dubovik et al. 2006). The nominal wavelengths of the almucantar inversion retrievals
333 are 440, 675, 870 and 1020 nm. An additional advantage of the AERONET database is that the
334 retrieval values are obtained consistently – the calibrations, corrections, QC and algorithms are
335 applied identically for each AERONET location.

336
337 For Version 2 AERONET data, there are different levels of AERONET data available for
338 download from the AERONET website. Level 1.0 is unscreened data while Level-1.5
339 undergoes automated cloud-screening (Smirnov et al., 2000). Level-2 represents data with pre-
340 field and post-field calibrations applied, manual inspection, and quality assurance (Smirnov et
341 al., 2000). In addition to the Level-1.5 screening, the criteria for Level-2 almucantar inversion

342 products include a check of the sky residual error as a function of AOD₄₄₀, solar zenith angle
343 must be greater than or equal 50 degrees, and almucantars must have a minimum number of
344 measurements in each of the four designated scattering angle bins. Further, for Level-2
345 absorption-related products (including SSA, AAOD, AAE, and the complex refractive index) the
346 AOD₄₄₀ must be greater than 0.4 to exclude more uncertain aerosol absorption estimates
347 (Holben et al., 2006). Version 3 AOD products are now available but the Version 3 inversion
348 products are not.

349
350 The AAOD values reported in the AERONET almucantar inversion files are obtained using the
351 relationship: $AAOD=(1-SSA)*AOD$. Schafer et al. (2014) has a nice description of how SSA is
352 obtained from the AERONET measurements. In the present study, in order to maximize the
353 number of AERONET data points available for comparison with the in-situ measurements,
354 Level-1.5 retrievals of AAOD and SSA were included in the analysis if there was a
355 corresponding valid Level-2 AOD value (i.e., the same primary criterion as was used in Bond et
356 al. (2013)). We will refer to these AAOD and SSA values as 1.5* data.

357 2.3 Merging the IN-SITU and AERONET data sets

358 Merging of collocated (within 15 km), but temporally disparate data sets can induce
359 discrepancies in the combined data set. Lag-autocorrelation analysis (e.g., Anderson et al.,
360 2003) is used to determine an appropriate time window for comparison of the AERONET and in-
361 situ profile measurements. Figure 2 shows that, at the surface, at both BND and SGP,
362 scattering is well correlated ($r(k)>0.8$) out to 4-5 hr lag, while absorption is less correlated than
363 scattering ($r(k)$ for absorption is 0.75 at BND and 0.55 at SGP). Based on the correlograms,
364 AERONET retrievals were merged with the in-situ profile data when the retrievals were within
365 +/-3 h of the end of the in-situ profile. This is the same time range constraint used to compare
366 AERONET and PARASOL SSA values (Lacagnina et al., 2015). Additionally, Figure 2
367 represents the maximum correlation that we can realistically expect to achieve in a comparison
368 of two different instruments with temporally offset measurements and provides context for the
369 AERONET/in-situ comparisons presented in Section 3.

370 Because the profiles are “stair-step” descents from ~4600 m asl down to ~450 m asl (e.g., see
371 Figure 4 in Sheridan et al., 2012), matching with AERONET retrievals at the end of the profile
372 means that the matches are more closely aligned with when the airplane is in the boundary
373 layer and thus, typically, sampling the highest aerosol concentrations. This way the maximum
374 time difference between the boundary layer portion of the flight and the AERONET retrieval is 3
375 h; if we’d chosen to match based on the start of the flight the maximum time difference between
376 the boundary layer measurements and the AERONET retrieval could be as large as 5 h. The
377 boundary layer portion (<1800 m asl) of the ~2 h profile takes approximately 30 min. While the
378 +/- 3 h match window was chosen based on the surface in-situ aerosol lag-autocorrelation
379 statistics (Figure 2), other time windows were also examined. For time windows less than +/-3 h
380 (e.g., 1 h and 2 h) the fit coefficients (slope, intercept) did not change significantly although the
381 AOD and AAOD correlation coefficients did improve for those smaller time windows. For time
382 windows longer than +/- 3 h (e.g., 6 h and 12h) there were changes in AOD and AAOD fit
383 parameters and the correlation coefficients decreased significantly. For SSA there appeared to

384 be no correlation between AERONET retrievals and in-situ calculated values regardless of
385 match window length (highest SSA correlation coefficient was 0.12, but most were less than
386 0.05 for both sites). The poor correlations for SSA are not surprising given the uncertainties at
387 low loading. The AERONET/in-situ comparisons for the +/-3 h window are discussed in section
388 3.1 below.

389 2.4 Uncertainties in IN-SITU and AERONET data

390 In any study comparing parameters obtained from different instruments and/or methods, an
391 understanding of the uncertainties in each of the parameters being compared is critical. Below
392 we discuss the uncertainties inherent in both the in-situ and AERONET datasets.

393 2.4.1 IN-SITU uncertainties

394 Uncertainties for measurements by the in-situ instruments have been described previously (e.g.,
395 Sheridan et al., 2002; Formenti et al., 2002; Shinozuka et al., 2011; Sherman et al., 2015) so
396 only an overview is provided here. Sheridan et al. (2002) calculated uncertainties in aerosol
397 light scattering for the TSI nephelometer to be 7-13% for 10 min legs depending on amount of
398 aerosol present – the higher uncertainty value applies to very low aerosol loadings (scattering <
399 1 Mm^{-1}). We assume that uncertainty in the profile scattering measurements is 13%. 13% is
400 appropriate for the higher altitude flight legs (10 min duration with, typically, low aerosol loading)
401 and is also reasonable for the lower altitude flight legs which are only 5 min in duration but have
402 significantly higher loading. At both BND and SGP the median boundary layer scattering is
403 typically $>10 \text{ Mm}^{-1}$ while median scattering for the upper altitude flight legs is typically between
404 $1\text{-}10 \text{ Mm}^{-1}$ (Andrews et al., 2011; Sheridan et al., 2012).

405
406 Unfortunately, because profile-specific aerosol hygroscopicity measurements were not available
407 for the in-situ aircraft measurements described here, a single hygroscopic growth
408 parameterization was applied for all profiles at each site as described in Section 2.1 and
409 equation 1. To determine the uncertainty in AOD induced by the uncertainty in the scattering
410 adjustment to ambient RH, AOD values were calculated using different γ values representing
411 the range of hygroscopic growth factors suggested by the aerosol chemistry. Specifically,
412 AOD_{440} was calculated for $\gamma \pm 1$ standard deviation and $\gamma \pm 2$ standard deviations. As described
413 above, γ was calculated from the climatological chemistry measurements made by the
414 IMPROVE network (14 years of data, ~1700 data points at BND; 10 years of data, ~1000 data
415 points at SGP) using the Quinn et al. (2005) parameterization. We calculated the mean and
416 standard deviation of γ based on those climatological chemistry measurements. Using this
417 approach, the uncertainty in AOD due to adjustment to ambient RH was determined to be
418 between 9% and 16%. This uncertainty might seem to be low, but recall that the 95th
419 percentiles of ambient RH values observed throughout the profiles were ~80% but that more
420 typically ambient RH in the boundary layer was less than 70% at BND and less than 60% at
421 SGP. Sum of squares uncertainty analysis suggests the overall uncertainty in the in-situ AOD is
422 approximately 30% for higher ambient humidities ($\text{RH}_{\text{amb}} > 70\%$) and approximately half that at
423 $\text{RH}_{\text{amb}} < 50\%$.

424

425 Jeong and Li (2010) have noted that the presence of nearby clouds may influence AOD values.
426 They've investigated the effect of high RH-halos embedded in aerosol layers that typically exist
427 in the vicinity of non-precipitating cumulus clouds. If the AERONET retrieval went through such
428 a halo it could result in an increased AOD due to the combined effects of hygroscopic growth,
429 cloud processing of aerosols and rapid gas-to-particle conversions. If the aircraft also flew
430 through this RH-halo then the effect would also be accounted for in the RH-corrected in-situ
431 measurements. However, if the high RH layer was between two flight levels then the aircraft
432 measurements would not account for it. Addressing this effect is outside the scope of this
433 paper.

434
435 The PSAP measurement of aerosol absorption is more uncertain than the aerosol scattering
436 measurements – PSAP uncertainty is reported to be in the 20-30% range (e.g., Bond et al.,
437 1999; Sheridan et al., 2002; Sherman et al., 2015). It should be noted that the PSAP absorption
438 measurement represents all absorbing aerosol collected on its filter, as opposed to being
439 specific to 'black carbon' absorption. That is actually helpful for this particular study as the
440 AERONET retrieval of AAOD also represents all flavors of absorption (e.g., 'black carbon',
441 'brown carbon' and dust). Müller et al. (2011) describe detailed experiments to characterize
442 filter-based absorption instruments and describe some additional limitations of the instruments.

443
444 There is, however, some question of whether the PSAP (or any filter-based measurement) is
445 able to accurately represent absorption by particles coated with semi-volatile or liquid organics,
446 due to the possibility of such coatings changing the characteristics of the filter substrate
447 (oozing!) after impaction (e.g., Subramanian et al., 2007; Lack et al., 2008). Comparisons of
448 filter-based absorption measurements for denuded and un-denuded particles (e.g., Kanaya et
449 al., 2013; Sinha et al., in revisions, 2017) suggest that the un-denuded particles have absorption
450 enhancements of 5-25% relative to those that have been through a denuder. These
451 comparisons show that stripping off coatings and evaporating the non-absorbing particles
452 reduces the measured absorption, i.e., that the effect of coatings is not completely lost in filter-
453 based measurements. The effect of coatings appears to increase the absorption value reported
454 by the PSAP relative to that reported by a non-filter-based instrument (Lack et al., 2008); in
455 other words the aerosol absorption values obtained from PSAP measurements may have a
456 positive bias. It is worthwhile to explore the potential magnitude of such a bias. The mean mass
457 concentrations of organic aerosol determined from the IMPROVE measurements near BND and
458 SGP (the OC_f value in the IMPROVE data set; Malm et al., 1994) are similar for both sites and
459 less than 2 $\mu\text{g}/\text{m}^3$, putting them firmly in the rural/remote category identified by Lack et al (2008;
460 their figure 4). Depending on whether figure 3 or figure 4 in Lack et al. (2008) is used, Lack et
461 al.'s (2008) results suggest that the PSAP might be overestimating absorption by a factor of 1.1
462 to 1.5 due to artifacts caused by organic aerosols. However, in a subsequent study, Lack et al.
463 (2012) reported a PSAP overestimate by factors of 1.02-1.06 over Los Angeles, considerably
464 lower than the Lack et al. (2008) results.

465
466 The positive bias in absorption related to filter-based measurements is the same order of
467 magnitude and direction of the absorption enhancement factor found by some lab and

468 theoretical studies for coated absorbing particles suspended in the atmosphere. Absorption
469 enhancement values of 1.3-3 have been predicted for coated particles (e.g., Bond et al., 2006;
470 Lack et al., 2009; Cappa et al., 2012) although enhancements larger than a factor of 2 have not
471 been measured for ambient aerosol (e.g., Lack et al., 2008; Cappa et al., 2012; McMeeking et
472 al., 2014). Wang et al. (2014) suggested that an absorption enhancement factor of 1.1 was
473 appropriate for fossil fuel influenced aerosol and that 1.5 was a more reasonable enhancement
474 factor for biomass burning affected aerosol. Biomass burning does not have a consistent
475 influence on either BND or SGP. Cappa et al. (2012) suggested that the discrepancies between
476 ambient and modelled and/or laboratory results, could be a result of differences in particle
477 morphology and/or chemistry. We have not made any adjustments for the absorption effects of
478 coatings or the potential positive bias in PSAP measurements as the science is still unclear.
479

480 In addition to the potential absorption enhancement due to organic coatings, it has been
481 suggested that aerosol water on absorbing particles may also enhance absorption. There have
482 been very few studies where the hygroscopic growth enhancement of absorption was explicitly
483 considered. Redemann et al. (2001) modeled absorption enhancement as a function of RH
484 based on characteristic atmospheric particles and found absorption enhancement values of up
485 to 1.35 at 95% RH; for the 95th percentile RH_{amb} values encountered at BND (78.9%) and SGP
486 (76.6%), the Redemann et al. (2001, their figure 2) study would predict absorption
487 enhancements of ~1.1. Nessler et al. (2005) and Adam et al. (2012) utilized both ambient
488 aerosol measurements and Mie theory to calculate absorption enhancement values due to
489 hygroscopic water uptake. Nessler et al. (2005) does not provide absorption enhancements as
490 a function of RH, but Adam et al. (2012) suggest absorption enhancements due to hygroscopic
491 growth of less than 1.1 at 80% humidity. Brem et al. (2012) report on laboratory studies that
492 show that aerosol absorption was enhanced by a factor of 2.2 to 2.7 at 95% relative humidity
493 relative to absorption at 32% relative humidity, although for RH less than ~80% (i.e., the RH
494 values observed in this study) they show no absorption enhancement (their figure 9). Lewis et
495 al. (2009) actually observe a decrease in absorption with increasing RH for some biomass fuels,
496 but hypothesize the decrease might have been due to their measurement technique and/or a
497 change in the morphology of the particles.
498

499 In summary, the positive bias in the PSAP measurements of aerosol light absorption might be
500 as high as a factor of 1.1 to 1.5 due to oozing (e.g., the overestimate of absorption reported by
501 Lack et al., (2008) for filter-based measurements). Atmospheric absorption may be
502 underestimated by PSAP measurements by up to a factor of 1.5 due to not accounting for
503 coating (organic or water) effects. Without additional laboratory and field measurements to
504 quantify the net effect of the possible positive and negative biases in PSAP measurements of
505 aerosol light absorption, it is not possible to estimate the actual uncertainty in the in-situ light
506 absorption measurements reported here due to coating effects. To address this, we double the
507 assumed PSAP uncertainty of ~25% to 50% in the calculations of uncertainty.
508

509 One aspect of the in-situ system that will affect both the scattering and absorption measurement
510 is the gentle heating used to dry the particle to RH<40%. The drying process we use (heating
511 of 40 C or less) may remove some volatile components but we believe the removal to be

512 minimal (<10-20%) based on lab and ambient volatility studies in the literature. Thermal
513 denuder studies suggest little removal of volatile components (<10%) at 40 C (e.g., Mendes et
514 al., 2016; Huffman et al., 2009, Bergin et al., 1997) although thermal denuders results may be
515 limited by short residence times (<20s). However, smog chamber evaporation studies on
516 ambient aerosol over longer time periods (minutes-hours) at ambient temperature also suggest
517 ambient aerosol may be less volatile than previously thought – Vaden et al. (2011) showed that
518 ambient SOA lost just ~20% of its volume after ~4h.

519
520 Once the uncertainties in the in-situ aerosol scattering and absorption are known, the
521 uncertainty in SSA ($SSA = \sigma_{sp} / (\sigma_{sp} + \sigma_{ap})$) can also be calculated. Formenti et al. (2002, their
522 equation 5) suggests the uncertainty in single scattering albedo ($\delta SSA / SSA$) can be calculated:

$$\delta SSA / SSA = (1 - SSA) * [(\delta \sigma_{sp} / \sigma_{sp})^2 + (\delta \sigma_{ap} / \sigma_{ap})^2]^{1/2} \quad (2)$$

523
524
525
526 For scattering uncertainties of 30%, (combined nephelometer and f(RH) induced uncertainty),
527 PSAP absorption uncertainties of 50%, and SSA values of 0.9, equation 2 results in an in-situ
528 SSA uncertainty of ~6% or approximately 0.06. For the higher altitude flight segments the
529 loading does tend to be quite a bit lower and thus has higher uncertainty but those upper-level
530 segments contribute little to the overall AOD or AAOD. Because the flight column SSA is
531 calculated using extinction-weighted SSA flight segments, segments with very low aerosol
532 concentrations will have little impact on the column SSA derived from the flight measurements.

533
534 In addition to instrumental uncertainties there are also uncertainties associated with the aircraft
535 flight patterns, i.e., the presence of aerosols below, between and above the discrete flight levels.
536 Missing aerosol above and below an aircraft profile is a potential issue in all aircraft/column
537 comparisons. Different approaches have been used to assess whether aerosol loading
538 contributions above the highest flight level (4.6 km asl) are important. Andrews et al. (2004)
539 utilized Raman lidar measurements to determine that 80-90% of the aerosol was below 3.7 km
540 asl at SGP (3.7 km was the maximum altitude flown by the original SGP airplane, although all
541 the profile flights utilized here occurred after the maximum flight level was increased to 4.6 km
542 asl). Andrews et al. (2004) also assumed an AOD contribution of 0.005 from
543 stratospheric aerosol which was not done here. At SGP, Turner et al. (2001) segregated lidar
544 aerosol extinction profiles by season and AOD. Their results (their Figure 1) suggest that for the
545 vast majority of cases observed at SGP, 5% or less of the extinction will be found above 4 km.
546 For low AOD cases ($AOD_{355} < 0.3$) their mean extinction profiles suggest little to no aerosol
547 extinction between 4-7 km. At BND, Esteve et al. (2012) noted that CALIPSO data indicated
548 negligible extinction above 4.6 km asl. Regionally, seasonal average profiles from CALIPSO
549 also suggest there is minimal aerosol above the flight's highest level (Ma and Yu, 2014; Yu et
550 al., 2010).

551
552 Although statistical profile results (e.g., Turner et al., 2001; Yu et al., 2010; Ma and Yu, 2014)
553 suggest little contribution from high altitude aerosol layers in the region of these two sites,
554 Schutgens et al. (2016) demonstrates the importance of considering the specifics rather than
555 the statistical. We used the Raman lidar best estimate data product of extinction profiles at

556 SGP to evaluate the presence of aerosol above the highest flight level at the site. For the SGP
557 in-situ profiles that had matches with AERONET inversion retrievals, we identified three lidar
558 profiles that exhibited aerosol layers at high altitudes, but in all three cases the presence of
559 these layers was also hinted at by an increase in the aerosol loading at the highest flight levels
560 of the in-situ measurement. Thus, we further screened in-situ/AERONET comparisons by
561 removing flights at SGP and BND with significant increases in loading at the highest flight levels.
562 There may still be aerosol layers above the level measured by the Raman lidar, but we have no
563 means of assessing that. The AOD comparison presented in Figure 3 suggests we are unlikely
564 to be missing significant aerosol at high altitudes.

565
566 Several papers (Andrews et al., 2004; Esteve et al., 2012; Sheridan et al., 2012) have shown
567 that there is a high correlation ($R^2 > 0.8$) between scattering measured at the surface site (SGP
568 or BND) with scattering measured at the corresponding lowest flight leg, although the slopes of
569 the relationships indicated that the airplane measurements might be missing a fraction (10-20%)
570 of the aerosol below about 150 m agl. Additionally, Esteve et al. (2012) found high correlation
571 (slope=1.01, $R^2 \sim 0.7$) between scattering AOD calculated by assuming the lowest leg
572 represented scattering in the entire layer between surface and that flight leg with scattering AOD
573 calculated from 1-sec data obtained during descent from the lowest flight leg to landing. This
574 result suggested that no consistent bias would result from assuming the lowest flight leg was
575 representative of the aerosol between surface and that altitude. We've looked at the
576 surface/lowest flight leg relationship specifically for the flights with matching AERONET
577 retrievals studied here. We found that at BND the surface and lowest level flight aerosol
578 measurements were virtually identical. At SGP the lowest level leg actually measured slightly
579 higher aerosol loading than was observed at the surface, which could lead to an overestimate of
580 the aerosol optical depth in that layer, depending on the shape of the profile.

581
582 Similarly, Esteve et al. (2012) investigated differences in aerosol scattering between and at flight
583 levels by comparing scattering AOD from the airplane descent between layers with that
584 calculated from the individual level legs in the profile. Again they were able to confirm that
585 measurements made during the fixed flight altitudes are representative of the aerosol near
586 those altitudes.

587 588 *2.4.2 AERONET uncertainties*

589 Uncertainties in AERONET retrievals have been reported in several papers. Eck et al. (1999)
590 indicate that the uncertainty in AOD is approximately 0.01 for a field-deployed AERONET
591 sunphotometer at solar zenith angle = 0 (i.e., sun directly overhead). For the almucantar
592 retrievals (solar zenith angle > 50) used here, the AOD uncertainty will be smaller as the
593 uncertainty in AOD decreases inversely with air mass (Hamonou et al., 1999; their equation 1).

594 Dubovik et al. (2000) report AERONET retrieved SSA uncertainties in their Table 4. For water
595 soluble aerosol (the predominant aerosol type at both BND and SGP) they report that SSA
596 values are reliable to within ± 0.03 when $AOD_{440} > 0.2$, while the uncertainty in SSA increases to
597 ($\pm 0.05-0.07$) for $AOD_{440} \leq 0.2$. The almucantar retrieval of SSA may be biased by errors in the
598 surface reflectance when the AOD is very low. Another potential issue is that the AERONET

599 retrievals report only one pair of (real, imaginary) refractive index values for the total size
600 distribution (for each wavelength). If there are two or more aerosol modes in the column, this
601 assumption may skew the resulting SSA and AAOD values, although the effect of such skewing
602 would depend on the aerosol properties and cannot be assessed here. Potential impacts in the
603 case of uneven mode absorption in the retrieved size distribution have been found to be minor
604 since the retrieved size distribution is more linked to forward scattering than absorption (pers.
605 comm., O. Dubovik).

606 Mallet et al. (2013) reports an AAOD uncertainty of 0.01 but does not indicate whether or how
607 the AAOD uncertainty would change with AOD_{440} . Using the sum of squares propagation of
608 errors to calculate the uncertainty in AAOD for both high and low AAOD cases results in an
609 AAOD uncertainty of approximately ± 0.015 for both high and low AOD cases (high $AOD_{440}=0.5$,
610 $\delta AOD=0.01$, $SSA=0.95$, $\delta SSA=0.03$, $AAOD=0.026$; low $AOD_{440}=0.2$, $\delta AOD=0.01$, $SSA=0.95$,
611 $\delta SSA=0.07$, $AAOD=0.011$). An AAOD uncertainty value of ± 0.015 suggests an uncertainty of
612 about 60% in AAOD for $AOD_{440}=0.5$ and more than 140% uncertainty in AAOD for $AOD_{440}<0.2$.

613 3. Results

614 In this section we first present comparisons of AOD, AAOD and SSA from the in-situ
615 measurements at BND and SGP with AERONET retrievals. This includes (1) direct
616 comparisons of each in-situ profile with contemporaneous AERONET retrievals; the BND and
617 SGP comparisons are then put in the wider context of a literature review of similar direct
618 comparisons of in-situ and AERONET AAOD and SSA; (2) seasonal comparisons of AOD,
619 AAOD and SSA from Phase II AeroCom model results, AERONET retrievals and in-situ
620 measurements for BND and SGP; and finally, (3) we discuss these results in the context of
621 biases in determination of AAOD.

622

623 *3.1.1 BND and SGP: in-situ vs AERONET – Direct Comparisons*

624 Figures 3, 4 and 5 show the direct comparisons of AOD, AAOD and SSA at both 440 nm and
625 675 nm. On all 3 plots, the blue points represent the same data set – each point indicates a
626 flight for which there was one or more successful AERONET Level-2 almucantar retrievals
627 within ± 3 hours of the end of the flight profile (if there was more than one retrieval
628 corresponding to a flight, the retrievals were averaged). The thin gray lines on the 440 nm plots
629 indicate the reported (AERONET) or calculated (in-situ) uncertainties in the data. Table 1
630 provides a comparison of the statistical values (median, mean and standard deviation) at 440
631 nm for each of the parameters at both of the sites for these direct comparisons (blue points in
632 Figures 3, 4, and 5). The low number of flights for which there are comparisons available ($\sim 10\%$
633 of total number of flights) indicate both the effects of AERONET stringent cloud screening
634 routine and the constraints imposed by the almucantar retrievals. In addition to limiting the
635 number of comparisons available for this study, this limited data availability also has implications
636 for modellers utilizing AERONET data – for example, Schutgens et al. (2016) has shown the
637 importance of temporal collocation in measurement-model comparisons. Figure 3 also contains
638 red points – the red data points represent all direct sun AERONET Level-2 AOD retrievals
639 during the ± 3 hours window around the end of each profile. Depending on atmospheric
640 conditions, there may be more than one AERONET retrieval within ± 3 hours of the end of each

641 profile, which is why in Figure 3 there are more red data points plotted than there are flights.
642 The red points have not been averaged in order to provide an indication of the variability in AOD
643 during the in-situ profiling flight.

644
645 The comparison between in-situ and AERONET AOD is important because it can be used to
646 evaluate how well the in-situ and AERONET retrievals can be expected to agree and, thus, set
647 the context for the AOD and SSA comparisons. Many studies have investigated the
648 relationship between in-situ and remotely sensed AOD (e.g., Crumeyrolle et al., 2014; Schmid
649 et al., 2009, and references therein). As noted in these studies, the in-situ derived AOD values
650 tend to be slightly lower than the AOD retrieved from remote sensing measurements. Figure 3
651 presents the comparison of Level-2 AOD for AERONET and in-situ measurements at 440 nm
652 and 675 nm for two sets of AERONET AOD data. The first comparison (red points on plots) is
653 for all direct sun AERONET Level-2 AOD measurements. The second comparison (blue points
654 on plots) is for flight-averaged AERONET Level-2 AOD measurements where all the criteria
655 required for almucantar retrievals are satisfied. Table 2 summarizes how many points make up
656 each of these data sets.

657
658 In general, Figure 3 shows that AERONET AOD tends to be higher than the in-situ AOD,
659 although there is good correlation between AERONET and in-situ AOD. The uncertainty bars
660 tend to overlap the 1:1 line suggesting that in-situ measurements provide a reasonable proxy of
661 the total column aerosol loading as represented by AERONET AOD. Student t-test evaluation
662 suggests that the AERONET and in-situ AODs are the same at the 95% confidence level. The
663 coefficients of determination (R^2) are within the range we would expect based on the lag-
664 autocorrelation of scattering at these two sites (Figure 2) and the +/-3 h time window. The R^2
665 values increase when sub-setted for the more restrictive Level-2 almucantar retrievals. The
666 lower in-situ AOD values observed at both sites, compared to AERONET, may be due to the
667 hygroscopicity adjustment from dry in-situ to ambient RH conditions being too low or
668 undersampling of larger particles (e.g., Esteve et al., 2012). Esteve et al. (2012) found slopes
669 closer to 1 when they restricted AERONET/in-situ AOD comparison to low ambient RH (<60%)
670 conditions, although the AERONET AOD values were still larger than the in-situ AOD. The
671 effect of undersampling larger particles or underestimating aerosol hygroscopicity on the AOD
672 and SSA comparisons are discussed in section 3.1.2. Some of the discrepancy between the in-
673 situ and the AERONET values may also be due to the limited vertical range covered by the
674 airplane (150 – 4200 m asl). We've excluded flights that might have had aerosol above the
675 highest flight level, based on Raman lidar comparisons (at SGP) and profile shapes (at BND).
676 The relationships observed between AERONET and in-situ AOD for both sites are very similar
677 to those observed for the recent DISCOVER-AQ campaign (e.g., Crumeyrolle et al., 2014, their
678 figure 3).

679
680 One thing to note on Figure 3a is the blue point marked BB (the BB stands for biomass
681 burning). This measurement occurred on June 28, 2006 and appears to have been strongly
682 affected by forest fire smoke transported from Canada. We applied the same hygroscopicity
683 adjustment to the measurements of this flight as we did to all of the BND flights and, in this BB
684 case, the hygroscopicity correction was the primary reason the in-situ AOD value is significantly

685 higher than the AERONET AOD value. This point would lie much closer to the 1:1 line if the in-
686 situ BB data were assumed to be hygroscopic. Previous work at the surface site at SGP has
687 shown that dust and smoke aerosol types tend to exhibit lower hygroscopicity than the
688 background aerosol normally observed at the site (Sheridan et al., 2001). This BB point
689 provides an extreme example of the downside of using a constant hygroscopic growth
690 parameter as a function of RH, although without additional information about the aerosol for
691 each profile it is difficult to do otherwise. The light blue dotted line on Figure 3 represents the
692 relationship between AERONET and in-situ data if the BB point is excluded.

693
694 Figure 4 presents the comparison of AAOD for flight-averaged AERONET and in-situ
695 measurements. As described above, the AERONET AAOD values shown in Figure 4 are what
696 we have termed Level-1.5* data – i.e., they are from Level-1.5 almucantar retrievals when there
697 was a valid Level-2 almucantar retrieval, but the $AOD_{440} > 0.4$ constraint was not applied. In
698 contrast to the AOD comparison depicted in Figure 3, the AERONET Level-1.5* AAOD values
699 are significantly higher than the in-situ AAOD values. Figure 4 also shows that the correlation
700 between the AERONET and in-situ AAOD is poorer than it was for AOD, particularly at BND (R^2
701 is 0.49 at BND and 0.68 at SGP for the 440 nm comparison). The lower correlation at BND is
702 somewhat surprising given the lag-autocorrelation results for aerosol absorption (Figure 2a) at
703 the BND surface site. Surprisingly, while the BND site has higher 3-hour autocorrelations for
704 absorption than SGP ($R = 0.75$ for BND and $R = 0.55$ for SGP, per Figure 2), the results for
705 BND in Figure 4 indicate less correlation than at SGP for absorption. Nonetheless, the
706 correlation coefficients for BND in Figure 4 ($R^2 = 0.49$ (blue) and 0.37 (red) correspond to $R =$
707 0.70 (blue) and 0.61 (red)) are not that far from the 3 h auto-correlation of $r(k=3h) = 0.75$ for
708 absorption at BND in Figure 2. For AAOD the uncertainty bars, while wider, exhibit significantly
709 less overlap with the 1:1 line (indeed no overlap at SGP) and indeed the student t-test suggests
710 the AERONET and in-situ AAOD values are different at the 95% level at both sites.

711
712 Both Figure 4 and the median values provided in Table 1 indicate that AERONET Level-1.5*
713 AAOD tends to be larger than the in-situ AAOD, although the scatter in the relationships
714 (particularly at BND) suggests that a multiplicative factor doesn't represent the relationship very
715 well. The purple points in Figure 4 indicate AAOD retrievals where the flight-averaged
716 $AOD_{440} > 0.2$. There is no obvious improvement of the relationship between in-situ and
717 AERONET AAOD when these points are considered (although there are only 1-4 comparison
718 points above $AOD_{440} > 0.2$ for each site).

719
720 The AAOD comparisons at 675 nm at BND (Figure 4c) are quite similar to those at 440 nm,
721 suggesting that there is little contribution to absorbing aerosol from dust, organic carbon and/or
722 NO_2 . In contrast, at SGP, there is a change in the relationship between AERONET and in-situ
723 AAOD from 440 to 675 nm indicating that one or more of these components may affect the 440
724 nm comparisons at that site (Figure 4d). Ångström exponent values from the matched
725 AERONET and in-situ profile data do not support the presence of dust, while the rural nature of
726 the site suggests significant levels of NO_2 are unlikely. Thus the most likely explanation is the
727 presence of organic carbon, although the IMPROVE sulfate and organic data used to estimate
728 aerosol hygroscopicity do not support this. The IMPROVE measurements tend to suggest a

729 relatively small contribution of organics to the aerosol mass with the average mass
730 concentration of organics only 40 to 60% that of sulfate aerosol mass concentration for BND
731 and SGP, respectively. In contrast, the Aerosol Chemical Speciation Monitor (ACSM)
732 measurements by Parworth et al. (2015) indicate that, depending on the month, organic aerosol
733 can contribute up to 70% of the total aerosol mass at SGP.

734

735 Figure 5 presents the comparison of column SSA retrieved from flight-averaged AERONET
736 inversions (Level-1.5* data) with the column SSA calculated from in-situ profile measurements
737 of aerosol scattering and absorption at BND and SGP. Consistent with the AOD and AAOD
738 comparisons (Figures 3 and 4) the SSA retrieved from AERONET tends to be much lower than
739 the SSA calculated from the in-situ profile measurements. As with AAOD, the SSA uncertainty
740 bars exhibit little overlap with the 1:1 line and a student t-test suggests the AERONET and in-
741 situ SSA values are different at the 95% level for both BND and SGP. At both sites the range in
742 AERONET-retrieved SSA is much wider than the range in column SSA obtained from the in-situ
743 profiles. Long term, in-situ measurements at the BND and SGP surface sites yield mean SSA
744 values of 0.92 and 0.95 respectively (Delene and Ogren, 2002, based on monthly-averaged
745 data). Delene and Ogren's (2002) surface SSA values are reported at low RH (RH<40%) and
746 550 nm; adjusting them to ambient conditions and 440 nm would likely cause them to increase
747 making them more comparable to the in-situ column SSA depicted in Figure 5 but even less like
748 the AERONET Level-1.5* SSA values. As with Figure 4, the purple points on Figure 5 indicate
749 when the flight-averaged $AOD_{440} > 0.2$; although there aren't enough points to draw a robust
750 conclusion, there does not appear to be an improvement in the relationship between in-situ and
751 AERONET SSA when only these purple points are considered.

752

753 Figure 5 also includes a set of 'hybrid SSA' (SSA_{hybrid}) points in yellow. These points have been
754 calculated using the AERONET AOD and the in-situ AAOD:

$$755 \quad SSA_{\text{hybrid}} = (AOD_{\text{AERONET}} - AAOD_{\text{PSAP}}) / AOD_{\text{AERONET}} \quad (3)$$

756 This hybrid approach to SSA eliminates the uncertainty associated with the empirical
757 hygroscopic growth factors applied to the in-situ scattering measurements, and also removes
758 the scattering uncertainty associated with undersampling the coarse mode. It does not,
759 however, eliminate the uncertainties associated with assuming the absorbing aerosol is
760 hygrophobic, that there is little absorption in the potentially undersampled coarse mode, or the
761 unknown contribution from absorption enhancement. SSA_{hybrid} is very similar to the SSA derived
762 from in-situ measurements, suggesting the primary discrepancy between the AERONET SSA
763 and the in-situ SSA is due to the determination of the absorbing nature of the aerosol, either due
764 to issues with the limitations of the filter-based measurements or to the interpretation of the
765 relative contribution of aerosol absorption from the AERONET inversion retrieval products.

766

767 *3.1.2 How might in-situ hygroscopicity assumptions and under-sampling of the aerosol affect*
768 *SSA and AAOD comparisons?*

769 Figure 3 shows that the AERONET AOD may be slightly larger than the in-situ AOD, while
770 Figures 4 and 5 suggest that the AERONET retrievals significantly overestimate the amount of
771 absorbing aerosol (low SSA, high AAOD) relative to the in-situ measurements. The slight

772 deviation between in-situ and AERONET AOD may lead to questions about whether directly
773 comparing other AERONET and in-situ parameters (e.g., SSA, AAOD) is a reasonable thing to
774 do and whether the AAOD and SSA comparisons shown in Figures 4 and 5 are related to
775 issues with the AOD comparison. As mentioned above, Esteve et al. (2012) suggested the
776 AOD difference was most likely due to either underestimating the hygroscopic growth correction
777 and/or undersampling of supermicron particles by the aircraft inlet. In this section we evaluate
778 how these two possible causes of the AOD discrepancy might affect the SSA and AAOD
779 comparisons.

780 Increasing the hygroscopic growth adjustment of the in-situ measurements would enhance the
781 in-situ scattering values used to calculate the in-situ AOD, but would not change the in-situ
782 AAOD because the absorbing particles are assumed to be non-hygroscopic. Consequently, the
783 comparison depicted in Figure 4 would not change with a different adjustment for hygroscopic
784 growth. Increasing the in-situ AOD, without affecting the in-situ AAOD, would result in higher in-
785 situ SSA values and an even greater discrepancy between AERONET and in-situ SSA values
786 than shown in Figure 5. To evaluate the effect of assuming absorbing particles were non-
787 hygroscopic, a sensitivity test was performed assuming the absorption enhancement due to RH
788 was the same as the hygroscopicity scattering enhancement, i.e., $\sigma_{ap}(RH_{amb})/\sigma_{ap}(RH_{dry})=a^*(1-$
789 $(RH_{amb}/100))^{-\gamma}$. While this is likely an extreme assumption, it had minimal effect on the
790 comparisons of AOD, AAOD and SSA.

791
792 The other likely candidate to explain the in-situ AOD being slightly lower than the AERONET
793 AOD is aircraft under-sampling of super-micron aerosol particles due to the 5 μm inlet cutoff'.
794 Esteve et al.'s (2012) comparison of column in-situ and AERONET scattering Ångström
795 exponents at BND suggested that the airplane measurements might be under-sampling larger
796 particles. Sheridan et al. (2012) estimated that the aircraft inlet 50% cut-off aerodynamic
797 diameter is approximately 5 μm , so particles larger than that are unlikely to be sampled by the
798 in-situ measurements but will be sensed by the AERONET sunphotometer. If we take into
799 account that atmospheric particles are likely to have a density greater than 1 g cm^{-3} , the actual
800 cut size would be closer to 3 or 4 μm . The AERONET volume size distributions were used to
801 estimate the fraction of column extinction due to particles less than 3 μm . At BND the mean and
802 standard deviation of the 3 μm extinction fraction ($\text{extinction}(D<3\mu\text{m})/\text{extinction}(D<30\mu\text{m})$) was
803 0.93 ± 0.07 , while at SGP the extinction fraction value was 0.88 ± 0.09 . At the BND and SGP
804 surface sites, most (80-90%) of the observed sub-10 μm scattering and absorption is also
805 attributed to sub-micron aerosol, with absorption more likely to be in the sub-micron size range
806 than scattering (Delene and Ogren, 2002; Sherman et al., 2015). This is consistent with the
807 observation that absorbing aerosol tends to be concentrated in sub-micron particles for typical
808 aged continental air masses (e.g., Hinds, 1982). Based on these observations, larger and
809 primarily scattering particles are more likely to be under-sampled by the in-situ measurements
810 than absorbing particles. This is the opposite of what is needed to explain the discrepancies
811 between AERONET and in-situ AOD, AAOD, and SSA shown in Figures 3-5. The in-situ
812 measurements would need to preferentially under-sample absorbing aerosol relative to
813 scattering aerosol in order to come into line with the AERONET observations. Additionally,
814 Sheridan et al. (2012) calculated particle transmission losses from behind the sample inlet on

815 the airplane to both the nephelometer and PSAP to be similar and to be less than 10% in the
816 particle diameter range $0.01 < D < 1 \mu\text{m}$. This suggests that preferential losses of absorbing
817 aerosol are also unlikely to occur downstream of the aerosol inlet. In summary, we can only see
818 two ways that the in-situ measurements can sample aerosol efficiently enough to represent
819 AERONET AOD fairly well but significantly underestimate AAOD and overestimate SSA: (1) not
820 accounting properly for the effect of coatings (organic or water) on absorption enhancement
821 which we've discussed in detail in the manuscript and (2) not sampling layers of predominantly
822 absorbing aerosol below, between, and/or above the flight layers. We suspect that the SSA
823 required of such layers in order to explain the AAOD and SSA discrepancies is physically
824 impossible.

825 3.2 Literature survey: in-situ vs AERONET – Direct Comparisons

826 Direct comparisons at BND and SGP suggest that AERONET retrievals underestimate SSA
827 and, consequently, that AERONET overestimates AAOD relative to in-situ measurements of
828 AAOD for the low AOD conditions typical at these two sites. The next question to address is
829 whether this discrepancy, found for two rural, continental sites in the central US with relatively
830 low aerosol loading, is more widely observed for direct in-situ/AERONET comparisons at a
831 variety of sites/conditions. As in section 3.1, the focus in this section is on direct comparisons of
832 column-averaged SSA (or AAOD) derived from in-situ measurements made during aerosol
833 profiling flights that were flown in close proximity (temporal and spatial) to an AERONET
834 retrieval. Tables 3 and 4 summarize literature results describing the direct comparisons of
835 AERONET retrievals with in-situ aerosol profile measurements for AAOD and column SSA.
836 Figure 6 provides a graphical overview of the SSA comparisons described in Table 4. Tables 3
837 and 4 and Figure 6 also include the BND and SGP comparisons described in this study. With
838 the possible exception some of the profiles reported by Corrigan et al. (2008), the literature
839 comparisons cited in Tables 3 and 4 and shown in Figure 6 have been made at higher AOD
840 conditions ($\text{AOD}_{440} > 0.3$) to reduce retrieval uncertainty. In contrast, the SGP and BND
841 comparisons are more representative of global AOD (Figure 1) with the majority of the
842 comparisons at BND and SGP occurring for $\text{AOD}_{440} < 0.2$. Please note that some of the earlier
843 studies shown in Figure 6 and described in Table 4 used values from Version 1 AERONET
844 Level-2.0 data. Where that was the case, we retrieved Version 2 AERONET Level-2.0 data
845 from the AERONET website and those Version 2 data are what is reported in Table 4 and
846 depicted in Figure 6. The comments section of Table 4 mentions the cases where this was
847 done. For some of these references we also retrieved the AOD_{440} values from the AERONET
848 website as the AOD_{440} values weren't reported in all papers.

849
850 Tables 3 and 4 have been restricted to studies with direct comparisons of column-averaged
851 AAOD or SSA retrieved from full in-situ vertical profiles flown near (within ~100 km) AERONET
852 sites within a few hours of the AERONET retrieval, i.e., studies that are comparable to the BND
853 and SGP studies described in Section 3.1. For non-plume data sets, Anderson et al. (2003)
854 found autocorrelations ≥ 0.8 at 100 km (their figure 6). For plume-influenced data sets they
855 found autocorrelations ~ 0.6 . Included in the tables are the field campaign name (if applicable),
856 number of AAOD or SSA comparisons, the primary type of aerosol studied, summary of AOD
857 comparisons (if available), altitude range covered by the airplane, instruments and data

858 processing (e.g., instrument corrections, treatment of hygroscopicity, wavelength adjustment)
859 and a summary of the results of the AOD comparison. The last column in Tables 3 and 4
860 includes information on the spatial and temporal differences between the in-situ measurements
861 and AERONET retrievals and comments on treatment of the AERONET and in-situ data. The
862 last column also notes how each campaign dealt with aerosol below and above the in-situ
863 profile if reported. It should be noted that the number of SGP and BND comparisons of AOD
864 and SSA in Tables 3 and 4 are only possible because we've utilized AERONET retrievals below
865 the recommended threshold of $AOD_{440} > 0.4$. The uncertainty for the BND and SGP
866 comparisons is much higher than for some of the other direct comparisons due to the low AOD
867 conditions observed at these sites.

868

869 For the three AOD closure studies listed in Table 3 (the BND and SGP results presented here,
870 plus results from a field campaign over the Indian Ocean) the AERONET retrievals indicate
871 more absorbing aerosol in the column than is suggested by the corresponding in-situ
872 measurements. The Corrigan et al. (2008) paper mentioned in Table 3 is the sole
873 AERONET/in-situ AOD comparison cited by Bond et al. (2013), as it was the only published
874 direct AOD comparison available. Corrigan et al. (2008) present no AOD comparisons that
875 could provide an indication of their sampling system efficiency, and information about the
876 wavelength of the comparisons and profiles specifics are lacking. To our knowledge, no other
877 direct comparisons of in-situ and AERONET AOD are available in the literature.

878

879 The SSA comparison studies listed in Table 4 and visually summarized in Figure 6 indicate that,
880 even at higher AOD, AERONET retrievals tend to indicate more-absorbing aerosol (lower SSA)
881 relative to in-situ measurements. While much of the observed difference between $SSA_{in-situ}$ and
882 $SSA_{AERONET}$ may fall within the uncertainty of the SSA values, as noted in Schafer et al. (2014),
883 the fact that the difference ($SSA_{AERONET} - SSA_{in-situ}$) is predominately negative across all the
884 direct comparisons found in the literature is not what would be expected from random error.
885 Figure 6 also shows the mean and 2*standard deviation of all of the points (black square and
886 vertical lines) and just the literature value points (black diamond and vertical lines). Based on
887 the characteristics of a normal distribution the standard deviation lines suggest ~80% of the
888 points will be negative – random error would suggest only 50% of the points should be negative.
889 Figure 6 suggests that AERONET retrievals of SSA could perhaps be used at $AOD_{440} < 0.4$,
890 perhaps down to $AOD_{440} \sim 0.25$ or ~ 0.3 – even at those low AOD values the differences in SSA
891 between AERONET and in-situ still tend to be within the AERONET uncertainty. However, as
892 Figure 6 shows, there are not a lot of direct comparisons to support such a choice.

893

894 Most of the SSA comparisons in Table 4 found fairly good agreement between AERONET and
895 in-situ AOD, suggesting that the issue is an over-estimation of the absorption contribution to
896 AOD rather than an underestimation of the AOD scattering contribution. This is consistent with
897 the AERONET AOD values being greater than those obtained from in-situ measurements
898 presented in Table 3. Out of the 63 profiles compared in Table 4, there are four exceptions,
899 (three from Leahy et al. (2007) and one from this study for the BND site) where $SSA_{AERONET}$ is
900 larger than the corresponding $SSA_{in-situ}$. Interestingly, the three exceptions from Leahy et al.

901 (2007) were for their high AOD ($AOD_{550} > 0.6$) cases; for their two low AOD ($AOD_{550} < 0.3$) cases
902 the opposite was found, i.e., $SSA_{AERONET} < SSA_{in-situ}$.

903
904 In summary, the literature survey featuring measurements across the globe for many aerosol
905 types suggests that even at higher AOD conditions, direct comparisons of AERONET with in-
906 situ aerosol profiles find that AERONET column SSA is consistently lower than the SSA
907 obtained from in-situ measurements (although often within the uncertainty of the AERONET
908 SSA retrieval and in-situ measurements). If there was no consistent bias in the AERONET/in-
909 situ comparison we would expect ($AERONET_SSA - INSITU_SSA$) to be evenly distributed
910 around zero. Instead, Figure 6, which summarizes the literature survey, suggests either that
911 AERONET retrievals are biased towards too much absorption, or that in-situ, filter-based
912 measurements of aerosol absorption are biased low. We note that the results from the literature
913 (e.g., Figure 6) indicate that the hypothesized low-bias in in-situ absorption is not associated
914 with a single airplane's measurement system or the atmospheric conditions encountered in a
915 single experiment. That leaves us with possible bias in the in-situ experimental methods
916 (instrument issues (nephelometer, PSAP), treatment of $f(RH)$, vertical coverage, sampling
917 artifacts), all of which we have attempted to address above.

918 An alternative explanation is that the AERONET SSA uncertainties are non-symmetric. Dubovik
919 et al. (2000) suggest that simulated retrievals of SSA for 'water soluble aerosol' are asymmetric
920 when different 'instrumental offsets' are assumed, particularly at lower AOD values (0.05 and
921 0.2). Their figure 4 shows a much larger decrease in SSA for some instrumental offsets relative
922 to the increase in SSA observed for an instrumental offset of the same magnitude but opposite
923 sign. Asymmetry is also indicated for 'biomass burning' aerosol (their figure 7) although the
924 asymmetry is in the opposite direction, i.e., the increase in SSA is larger than the decrease for a
925 given pair of instrumental offset values. It is not obvious from their figure 7 whether the retrievals
926 are asymmetric for simulated dust aerosol. Interestingly, at least three of the four points in
927 Figure 6 with $AERONET_SSA > INSITU_SSA$ represent retrievals of biomass burning aerosol.

928 3.3 BND and SGP: in-situ vs AERONET and AeroCom model output – Statistical Comparisons

929 Most of the statistical comparisons between AERONET and in-situ profiles (e.g., Ramanathan et
930 al., 2001; Leahy et al., 2007; Ferrero et al., 2011; Johnson et al., 2011) were for short-term field
931 campaigns with a limited number of in-situ profiles. The advantage of the multi-year, in-situ
932 vertical profiling programs at BND (401 flights) and SGP (302 flights) is that we can compare the
933 statistics for both in-situ and AERONET values as opposed to comparing individual in-situ
934 values to remote retrieval statistics. Figure 1 in Andrews et al. (2011) and Figure 9 in Sheridan
935 et al. (2012) demonstrate that the BND and SGP flight programs captured the multi-year
936 seasonality in aerosol properties at these two sites. Because of the large number of flights over
937 an extended period of time, Skeie et al. (2011) was able to compare the seasonally averaged,
938 in-situ absorbing aerosol profiles from BND and SGP with seasonal vertical profiles of black
939 carbon generated by the Oslo-CTM2 model. Skeie et al. (2011) found that the model
940 underestimated absorbing aerosol relative to the BND and SGP in-situ profiles for most seasons
941 and altitudes, although agreement between the model and measurements tended to be better at
942 higher altitudes.

943
944 As mentioned in the introduction, AERONET retrievals of AAOD have been used to suggest
945 upscaling factors for modelled values of absorbing aerosol (e.g., Sato et al., 2003; Bond et al.,
946 2013). These model/AERONET comparison studies are typically based on model and
947 measurement statistics (i.e., properties are averaged over time and region) rather than direct
948 comparisons due to both computational constraints and the discrete nature of the AERONET
949 measurements. Given the statistical nature of some historical AERONET/in-situ comparisons
950 as well as the typical model/AERONET comparison constraints, in this section we compare
951 monthly statistics for in-situ measurements, AERONET retrievals and AeroCom model output.
952 It should be reiterated here that we are comparing asynchronous data and that there
953 are some additional differences amongst the data sets that need to be kept in mind: the
954 AERONET data are rigorously cloud-screened (although cloud halo effects may persist
955 (e.g., Jeong and Li, 2010) and only obtained during daytime; the in-situ measurements
956 are also daytime-only and the airplane did not fly in-cloud due to FAA flight restrictions,
957 but may have flown near clouds; and the model data include day and night with clouds
958 and also represent values over a 1x1 degree grid.

959
960 Figure 7 shows the 440 nm monthly medians of AOD, AAOD and SSA at BND and SGP based
961 on the in-situ profile measurements, and two versions of AERONET retrievals as described
962 below. For the in-situ properties, all profiles were used, regardless of whether there was an
963 AERONET retrieval corresponding to the flight. The AERONET monthly medians in Figure 7
964 use the long-term (1996-2013) AERONET data record for each site. As described previously,
965 the lines labeled AERONET 1.5* were calculated from Level-1.5 inversion data with matching
966 Level-2 almucantar retrievals. The lines labeled AERONET 2.0 utilized only Level-2 almucantar
967 retrieval data. In both cases the median AERONET AOD values represent those Level-2 AOD
968 measurements for which there was also an AAOD and SSA retrieval, ensuring that the
969 AERONET AOD medians represent the same set of retrievals as the corresponding AAOD and
970 SSA medians in the figure. The AERONET Level-1.5* AOD monthly medians are representative
971 of the direct sun AERONET Level-2 AOD climatology at the two sites. Figure 7 also includes
972 the AeroCom Phase II model monthly medians for BND and SGP (Kinne et al., 2006, Myhre et
973 al., 2013) with model emissions, meteorology and other details briefly described in Myhre et al.
974 (2013). The AeroCom values, which were provided at 550 nm, have been adjusted to 440 nm
975 using the reported AeroCom monthly scattering Ångström exponent to adjust AOD wavelength
976 and assuming an absorption Ångström exponent of 1 for the AAOD wavelength adjustment. It
977 should be noted that the three monthly data sets (AERONET, AeroCom, and in-situ) plotted in
978 Figure 7 are derived from measurements for overlapping, but not identical time periods, i.e.,
979 these plots represent climatological comparisons rather than direct comparisons of the data
980 sets.

981
982 At both sites, the climatological seasonal patterns for AOD (i.e., high in summer, low in winter)
983 are similar for the three data sets: in-situ measurements, AERONET Level-1.5* retrievals (recall
984 that the AERONET 1.5* AOD is representative of the overall AERONET AOD climatology at
985 each site) and AeroCom model output. At BND the AeroCom model AOD tends to be larger

986 than the in-situ and AERONET 1.5* AOD values by up to a factor of two. AERONET 1.5* AOD
987 is larger than the in-situ AOD in the summer (by up to 50%) but quite close the rest of the year
988 (typically within 20%). At SGP the AOD monthly medians from in-situ measurements and
989 AERONET Level-1.5* are almost identical for August-December, with slightly more discrepancy
990 among the AOD values in summer and early part of the year. In contrast, AeroCom model
991 median AOD values tend to agree better with AERONET 1.5* and in-situ AOD values from
992 January-July but are noticeably higher (up to a factor of 2) in the later half of the year. At both
993 sites, the median AERONET Level-2 AOD values (corresponding to AAOD and SSA retrievals)
994 are much higher (by a factor of 2 or more) than the Level-1.5* and in-situ climatologies due to
995 the $AOD_{440} > 0.4$ constraint. During the cleanest, lowest humidity, and often cloudiest months of
996 the year (December-February) there are none to few Level-2 almucantar retrievals of SSA and
997 AAOD at either BND or SGP – the gray lines in Figures 7ab are lacking data points for Jan.,
998 Feb. and Dec. at BND and Jan. and Dec. at SGP.

999
1000 For AAOD at BND, the AeroCom model output falls between the AERONET 1.5* and in-situ
1001 values, with AERONET 1.5* AAOD being higher than the in-situ data by up to a factor of 8. As
1002 with AOD, the AERONET AAOD Level-2 values are much higher than the in-situ or modelled
1003 AOD values due to the constraint that they are only retrieved at high loading conditions
1004 ($AOD_{440} > 0.4$). The three data sets (AeroCom, in-situ and AERONET 1.5*) agree best in the
1005 month of May when the median values of AAOD are within 30%. At SGP there is fairly good
1006 agreement between AeroCom model and in-situ AAOD for the first 7 months of the year, while
1007 the AERONET 1.5* monthly AAOD values are considerably higher for that same time period.
1008 For the latter part of the year the in-situ AAOD values tend to be lower than both AERONET and
1009 AeroCom AAOD values.

1010
1011 The AERONET 1.5* SSA values tend to be quite a bit lower at BND, and somewhat lower at
1012 SGP, which is why the AERONET 1.5* AAOD values tend to be higher (recall that for
1013 AERONET data AAOD is calculated using $AAOD = (1 - SSA) * AOD$). Figure 7 also shows that the
1014 AERONET Level-2 SSA values are similar to the monthly in-situ and AeroCom SSA medians
1015 between April and November. There are no AERONET Level-2 almucantar retrievals of SSA in
1016 January or December at either site. For the February and March, median Level-2 almucantar
1017 retrievals of SSA are based on very few data points resulting in bigger discrepancies between
1018 AERONET Level-2 almucantar retrievals of SSA and the in-situ and AeroCom SSA values.

1019
1020 Aside from differences in magnitude, there are also differences in the seasonal patterns of AOD,
1021 AAOD and SSA for the three data sets (in-situ, AERONET 1.5* and AeroCom). For example, at
1022 BND, the AERONET and in-situ AAOD both have a bi-modal annual distribution with peaks in
1023 late spring and early fall, which is not captured by the AeroCom AAOD and which is not seen in
1024 the AOD seasonality. The observed seasonal differences may be a result of (a) the different
1025 climatology time ranges for each method and/or (b) very little overlap in the measurement times
1026 for AERONET and in-situ measurements or (c) in the case of the models, not capturing local
1027 emissions near the sites. This highlights the importance of direct (i.e., near in time and space)
1028 comparisons in order to understand these seasonal differences. The seasonal cycle plots in
1029 Figure 7 also direct attention to the fact that AOD and AAOD vary independently rather than

1030 exhibiting the same seasonal pattern. This suggests that different emission sources and/or
1031 atmospheric processes control the variability of absorption and scattering aerosol over the
1032 course of the year.

1033 1034 3.4 Discussion

1035 Because AERONET data are readily available and are being widely used as a benchmark data
1036 set for evaluating model output of AAOD (e.g., Chung et al., 2012; Bond et al., 2013; He et al.,
1037 2014; Wang et al., 2014) as well as for comparison with satellite retrievals and development of
1038 AAOD climatologies, we document and discuss some of the previous methods for utilizing
1039 existing AERONET retrievals that have been used to estimate AAOD at low AOD ($AOD_{440} < 0.4$)
1040 where Level-2 retrievals do not exist. These approaches fall into several categories (1) use only
1041 Level-2 data; (2) use Level-2 and Level-1.5 data with acknowledgement of greater uncertainty in
1042 the retrievals and potentially additional measurement constraints for the Level-1.5 data; (3)
1043 make climatological assumptions about the representativeness of Level-2 SSA for low AOD
1044 conditions to obtain AAOD.

1045 Clearly the simplest approach to minimize uncertainty in retrieved AERONET AAOD and SSA is
1046 to only use AERONET Level-2 retrievals which include the $AOD_{440} > 0.4$ constraint. This
1047 approach has been and continues to be used (e.g., Koch et al., 2009; Bahadur et al., 2010;
1048 Chung et al., 2012; Buchard et al., 2015; Pan et al., 2015; Li et al., 2015). However, as shown
1049 in Figure 1 the vast majority of the globe has $AOD_{440} < 0.4$, meaning few if any AERONET Level-
1050 2 AAOD or SSA retrievals will be available for most locations. This approach is quite useful in
1051 regions (or for case studies) with high aerosol loading (high AOD). However, excluding low
1052 loading conditions is likely to cause AERONET AAOD statistics to be biased high. This is
1053 particularly important when evaluating models in clean locations such as the Arctic. The
1054 $AOD_{440} > 0.4$ constraint may also affect the SSA statistics.

1055 Some studies have utilized AERONET Level-1.5 retrievals of absorption-related aerosol
1056 properties in order to avoid being limited to the high AOD levels required by Level-2 data (e.g.,
1057 Lacagnina et al., 2015; Mallet et al., 2013). These studies note that Level-1.5 data include more
1058 relevant AOD values but that there are accompanying higher uncertainties in the retrievals for
1059 absorption related properties. Mallet et al. (2013) use Level-1.5 data to evaluate the spectral
1060 dependence of aerosol absorption. Lacagnina et al. (2015) utilize both Level-2 and Level-1.5
1061 AERONET data in their comparison with PARASOL satellite retrievals of SSA and AAOD. For
1062 the Level-1.5 data they apply the additional requirement that the solar zenith angle must be
1063 $\geq 50^\circ$. Lacagnina et al. (2015) find quite good agreement (within ± 0.03) for AAOD and note
1064 that larger differences between PARASOL and AERONET retrieval occur at higher AOD
1065 conditions, possibly due to less homogenous aerosol (i.e., plumes).

1066 A more sophisticated approach to deal with SSA (and hence AAOD uncertainties) at low AOD is
1067 implemented by Wang et al. (2014). They make the assumption that SSA is independent of
1068 AOD (at least as a function of season) and utilize climatological Level-2 SSA values for each
1069 season with the measured AOD in order to obtain AAOD. The seasonal climatologies of SSA
1070 are based on 12 years of Level-2 AERONET data. For the two US continental sites studied in

1071 this paper, the approach of Wang et al. (2014) would likely minimize the potential AERONET
1072 tendency towards high AAOD at low AOD conditions as the Level-2 monthly climatological SSA
1073 values are quite similar to SSA values obtained by in-situ measurements (Fig. 7).

1074 A similar, though statistical, approach was used in Bond et al.'s (2013) bounding BC paper in
1075 order to reduce the uncertainty and better represent AERONET SSA and AAOD retrievals at
1076 low AOD. Bond et al. (2013) worked with AERONET monthly local statistics for the time period
1077 2000-2010. Monthly values of AAOD and SSA at 550 nm were calculated from size distributions
1078 and refractive index when there were at least 10 valid inversion retrievals for that month at that
1079 site in the 2000-2010 period (most sites had more than 10 retrievals in a given month over the
1080 11 year period). It was assumed in Bond et al. (2013), based on AERONET reported
1081 uncertainties, that the retrieved absorption-related values were more reliable at larger AOD and
1082 so they made some adjustments to account for this. For each site, AAOD and SSA values were
1083 binned as a function of AOD (there were five AOD bins, with each bin corresponding to 20% of
1084 the AOD probability distribution). For lower AOD conditions, the calculated AAOD and SSA
1085 values were replaced by values obtained during larger AOD conditions for the same month as
1086 follows: (i) the SSA and AAOD values corresponding to AOD_{550} of 0.25 were prescribed for all
1087 SSA and AAOD observations at lower AOD and (ii) for locations where all $AOD_{550} < 0.25$, the
1088 average SSA and AAOD of the upper 20th percentile of AOD observations at the site was
1089 prescribed for all lower AOD bins. Finally, the average of all five bins was used to determine the
1090 overall monthly average. In the case of AAOD the bin averages were simply averaged to get
1091 the monthly value while for SSA the AOD-weighted bin averages were averaged to get the
1092 monthly value. Note: the $AOD_{550}=0.25$ cutoff point used in Bond et al. (2013) corresponds
1093 (approximately) to $AOD_{440}=0.35$ for smaller particles and $AOD_{440}=0.25$ when large particles are
1094 present. Thus it is less strict than the AERONET recommended constraint of $AOD_{440} > 0.4$, but it
1095 had been suggested that the recommended constraint might be too restrictive (pers. comm., O.
1096 Dubovik).

1097 One drawback affecting approaches using climatological values of SSA (e.g., Wang et al., 2014;
1098 Bond et al., 2013) is that they may not account for the systematic variability that has been
1099 observed between SSA and loading at many sites, although AOD is usually more variable than
1100 the composition (or SSA). Still some studies with in-situ data (e.g., Delene and Ogren, 2002;
1101 Andrews et al., 2013; Pandolfi et al., 2014; Sherman et al., 2015) indicate that SSA
1102 systematically decreases with decreasing aerosol loading. A similar SSA/AOD systematic
1103 variability relationship is also observed at some North American AERONET sites. Schafer et al.
1104 (2014; their figure 6) shows SSA decreasing at lower loading for the GSFC site near
1105 Washington D.C. during the period of their field campaign; they also show similar relationships
1106 between SSA and AOD based on the long-term data for three mid-Atlantic AERONET sites.
1107 Additionally, a quick survey (not shown) of other long-term North American AERONET sites with
1108 good statistics (i.e., lots of points) for Level-1.5 SSA retrievals (e.g., Billerica (Massachusetts),
1109 Bratts Lake (Saskatchewan, Canada), COVE (Virginia), Egbert (Ontario, Canada), Fresno
1110 (California), Konza (Kansas), SERC (Maryland), and University of Houston (Texas)) indicates
1111 this systematic relationship may be observed at a wide range of locations in North America.
1112 Such climatological analyses may mask short-lived and/or infrequent aerosol events (e.g., dust
1113 or smoke incursions) that may have significantly different optical properties.

1114 Figure 8 shows the systematic relationships between SSA_{440} and AOD_{440} for BND and SGP for
1115 both the AERONET retrievals and in-situ profile measurements. Consistent with previous
1116 figures, we have utilized SSA values for $AOD_{440} < 0.4$ when there was a valid Level-2 AOD
1117 inversion retrieval, i.e., what we call AERONET Level-1.5*. Also included on the figure is a line
1118 showing the SSA_{550} versus scattering ($\sigma_{sp,550}$) relationships for the surface measurements at
1119 BND and SGP. The surface measurements are made at low RH conditions ($RH < 40\%$) and
1120 adjusted to ambient RH using the available meteorological measurements at the site (ambient
1121 RH at 2 m at SGP and ambient RH at 10 m at BND); adjustment of the surface measurements
1122 from dry to ambient conditions shifts the SSA_{550} values upward (assuming absorption is not
1123 affected) and the scattering values to the right.

1124
1125 Figure 8 suggests that for all three sets of measurements at both sites, there is a consistent
1126 decrease in SSA as aerosol loading decreases below $AOD_{440} = 0.2$. This relationship implies
1127 that a climatology based on SSA values measured at high AOD may underestimate the AOD
1128 climatology. The AERONET SSA values are lower than the in-situ profile values as would be
1129 expected from the results presented in sections 3.1 and 3.3. The AERONET SSA values are
1130 also lower than the surface in-situ SSA values – the surface in-situ SSA values adjusted to
1131 ambient conditions are quite similar to those obtained from the in-situ vertical profiles. It should
1132 however be noted that despite the discrepancy between in-situ and AERONET SSA values,
1133 Figure 8 shows that the SSA values for all three sets of measurements at SGP are within the
1134 reported AERONET SSA uncertainty range of 0.05-0.07 for $AOD_{440} < 0.2$ across the narrow and
1135 low AOD range shown in the figure. At BND the SSA values are within the AERONET SSA
1136 uncertainty range down to $AOD_{440} \sim 0.1$. At the lowest AOD values ($AOD_{440} < \sim 0.05$) the
1137 AERONET SSA values diverge, consistent with very large uncertainties expected in the
1138 AERONET SSA retrievals in the cleanest conditions. Uncertainty in the AERONET AOD
1139 retrieval may begin to affect the AERONET SSA retrieval where ± 0.01 AOD uncertainty is
1140 equivalent to a 20% change in AOD for AOD of 0.05. In addition, at such low AOD values, the
1141 surface reflectance uncertainties may influence AERONET's retrieval of SSA. Figure 8
1142 suggests that, in terms of the shape of the systematic variability plot, there are no obvious
1143 retrieval issues for AERONET SSA retrievals in the range $0.05 < AOD_{440} < 0.2$, although this is in
1144 the AOD range where high uncertainty in the SSA retrieval is expected (Dubovik et al., 2000).

1145
1146 There are large differences (orders of magnitude) in the number of data points in each of the
1147 data sets; the number of points in each bin is indicated by the color-coded histograms shown on
1148 Figure 8. The mean standard error (MSE) in SSA ($MSE = (\text{standard deviation}) / (\text{number of}$
1149 $\text{points})^{1/2}$) is indicated by the shading surrounding the solid colored lines. The MSE is quite
1150 similar for the AERONET 1.5* and in-situ profile measurements across the AOD range plotted in
1151 Figure 8, suggesting the observed systematic variability is not merely due to small numbers of
1152 data points in each bin, particularly at lower loading. However, the fact that the AERONET MSE
1153 is approximately the same as the in-situ profile MSE, despite having approximately an order of
1154 magnitude larger number of points/bin, indicates that variability in the retrieved AERONET SSA
1155 is larger than the variability in SSA derived from in-situ profile measurements.

1156 This study has utilized a valuable but spatially limited (i.e., two rural continental North American
1157 sites) climatological vertical profile dataset to explore AERONET retrievals of AAOD and SSA.
1158 Clearly, one way to address the observed discrepancy between in-situ and AERONET AAOD is
1159 to pursue a focused measurement program designed to acquire statistically robust in-situ
1160 vertical profiles over AERONET sites representing a wide range of conditions and aerosol types.
1161 This type of measurement program has been proposed to evaluate satellite retrievals and better
1162 characterize atmospheric aerosol (R. Kahn, SAM-CAAM, pers. comm.). Further evaluation and
1163 development of in-situ instrumentation for measuring aerosol absorption is also necessary,
1164 particularly in assessing the effects of coatings and hygroscopicity on the resulting absorption
1165 values. Additional evaluation of the AERONET retrieval algorithm may provide insight into a
1166 potential SSA and, thus, AAOD bias (e.g., Hashimoto et al., 2012). The discrepancies reported
1167 here between in-situ and AERONET values of AAOD and SSA suggest that caution should be
1168 used in upscaling model results to match AERONET retrievals of absorbing aerosol as this will
1169 have a significant impact on global radiative forcing estimates. The work of Wang et al. (2016)
1170 has shown that other factors (e.g., the spatial resolution of models and emissions) may also
1171 contribute to the differences observed between model and AERONET retrievals of AAOD.
1172 Thus, to really be able to understand and simulate the influence of absorbing aerosol on
1173 radiative forcing will require expanded effort on both the measurement and modeling fronts.

1174 4. Conclusion

1175 AERONET retrievals of SSA at low AOD conditions (below the recommended $AOD_{440} < 0.4$
1176 constraint) are consistently lower than coincident and co-located in-situ vertical profile
1177 observations of SSA (based on detailed comparisons at two rural sites in the US).
1178 Correspondingly, AERONET retrievals of AAOD at low AOD are consistently higher than those
1179 obtained from in-situ profiles. A survey of the literature suggests that even at higher loading
1180 ($AOD_{440} > 0.4$) AERONET SSA retrievals tend to be lower than SSA values obtained from vertical
1181 profiling flights, although discrepancies are within the reported uncertainty bounds down to ~
1182 $AOD_{440} > 0.3$. The tendency of AERONET SSA to be lower suggests either that AERONET
1183 retrievals over-estimate absorbing aerosol or that the in-situ measurements under-estimate
1184 aerosol absorption. Since the observed discrepancy in SSA can not definitively be attributed to
1185 either technique, the idea of scaling modelled black carbon concentrations upwards to match
1186 AERONET retrievals of AAOD should be approached with caution. If the AERONET SSA and
1187 AAOD retrievals are indeed biased towards higher absorption, such an upscaling may lead to
1188 aerosol absorption overestimates, particularly in regions of low AOD. If the discrepancy
1189 between the in-situ and AERONET AAOD is due to issues with the in-situ measurements of
1190 absorption, the only way we see to increase the in-situ absorption values is a significant
1191 enhancement (on the order of a factor of 2 or more) in absorption due to a coating effect. While
1192 that level of absorption enhancement factor is within the range suggested by modelling studies,
1193 it is significantly higher than many observations of absorption enhancement for ambient aerosol
1194 reported in the literature.

1195 The AERONET retrievals of SSA and AAOD have been used as a primary constraint on global
1196 model simulations of aerosol absorption. Using only Level-2 retrievals of AAOD (i.e., for
1197 $AOD_{440} > 0.4$) on a global scale (e.g., Koch et al., 2009; Bahadur et al., 2010; Chung et al., 2012;

1198 Buchard et al., 2015; Pan et al., 2015; Li et al., 2015) is likely to lead to significant over-
1199 estimates of absorption in cleaner regions although it may be appropriate for conditions of high
1200 loading. Several different approaches of varying complexity have been developed to better
1201 represent absorbing aerosol for cleaner conditions. Some of these approaches utilize SSA at
1202 high AOD to estimate AAOD at lower AOD conditions (e.g., Bond et al., 2013; Wang et al.,
1203 2014), while others utilize Level-1.5 retrievals with the added uncertainty that entails (e.g.,
1204 Lacagnina et al., 2015; Mallet et al., 2013). Based on the analysis presented here, we cannot
1205 say how to best estimate SSA or AAOD from AERONET retrievals for the low AOD conditions
1206 prevalent around much of the globe.

1207 Some in-situ measurements suggest that a systematic relationship exists between SSA and
1208 AOD, but these measurements are spatially sparse and typically not made at ambient
1209 conditions. Nonetheless, systematic relationships between SSA and AOD, similar to those seen
1210 in the in-situ data at the two sites, are also observed for multiple North American AERONET
1211 sites. The existence of such a systematic relationship may limit the accuracy of AAOD
1212 estimates when climatological values for SSA from high AOD retrievals are assumed to apply at
1213 low loading conditions. However, for the two mid-continental rural sites studied here, the
1214 statistically-based monthly medians of SSA from Level-2.0 inversions (i.e., SSA values derived
1215 for $AOD_{440} > 0.4$) appear to be quite consistent with monthly SSA values obtained from in-situ
1216 measurements and AEROCOM model simulations. This suggests that, at these two sites, using
1217 the Level-2.0 inversion SSA to retrieve monthly AAOD at lower AOD conditions (e.g.,
1218 $AAOD = AOD * SSA$) would not bias the resulting monthly AAOD high, as would occur if only
1219 AAOD values for high AOD cases are included in the AAOD statistics. . This may not be true
1220 for other locations or averaging times. Further, for these two sites, a more complex approach to
1221 retrieve monthly AAOD is needed for very clean months when no Level-2.0 inversions are
1222 available.

1223 This study points to several areas where additional research would be useful in resolving the
1224 observed AERONET/in-situ absorption-related discrepancies. First, continued laboratory, field
1225 and modelling efforts are needed to elucidate and unify the current inconsistencies in the
1226 literature on the effects of coatings on absorption enhancement reported for field and lab
1227 measurements and for model simulations. Second, a more extensive evaluation of the
1228 hygroscopicity of ambient (not lab-generated!) absorbing particles would be helpful. Third,
1229 better characterization of how filter-based measurements of absorption respond to coated
1230 particles would be useful, not just in the context of this study, but also for improving our
1231 understanding of the in-situ absorption data acquired by long-term, surface aerosol monitoring
1232 networks (e.g., GAW). Finally, the development of a focused measurement program designed to
1233 acquire statistically robust in-situ vertical profiles over AERONET sites representing a wide
1234 range of conditions and aerosol types could be used to explore the relationships between
1235 retrievals of column properties and variable aerosol profiles and to provide further validation of
1236 the inversion retrieval data products.

1237 **Acknowledgements**

1238 Funding for the SGP airplane measurements was provided by DOE/ARM, while the BND
1239 airplane measurements were funded by NOAA's Climate Program Office. Greenwood Aviation

1240 and FlightSTAR provided fabulous pilots and maintenance of the aircraft. Derek Hageman
1241 (University of Colorado) is owed much for his coding genius and Patrick Sheridan
1242 (NOAA/ESRL/GMD) for making instruments on both airplanes work and ensuring the quality of
1243 the BND aircraft data set. We thank the modelling groups for providing AeroCom Phase II
1244 results. We greatly appreciate the ease of access to and use of IMPROVE aerosol chemistry
1245 data for the Bondville and Cherokee Nation IMPROVE sites. IMPROVE data were downloaded
1246 from: <http://views.cira.colostate.edu/web/DataWizard/>. This study was supported by NOAA
1247 Climate Program Office's Atmospheric Chemistry, Carbon Cycle and Climate (AC4) program.
1248 BHS acknowledges funding by the Research Council of Norway through the grants AC/BC
1249 (240372) and NetBC (244141). Last, but not least, we also gratefully acknowledge the very
1250 helpful discussions from David Giles and Brent Holben from AERONET.

1251
1252

1253 **References**

- 1254 Adam M., Putaud, J.P., Martins dos Santos, S., Dell'Acqua, A., Gruening, C., "Aerosol
1255 hygroscopicity at a regional background site (Ispra) in Northern Italy," *Atmos. Chem. Phys.*,
1256 12, 5703–5717, 2012.
- 1257 Anderson, T. L., Charlson, R. J., Winker, D. M., Ogren, J. A., and Holmén, K., "Mesoscale
1258 Variations of Tropospheric Aerosols," *J. Atmos. Sci.*, 60, 119–136, 2003.
- 1259 Anderson, T. L. and Ogren, J. A., "Determining aerosol radiative properties using the TSI 3563
1260 integrating nephelometer," *Aerosol Sci. Technol.*, 29, 57–69, 1998.
- 1261 Andreae, M. O., Gelencsér, A., "Black carbon or brown carbon? The nature of light-absorbing
1262 carbonaceous aerosols," *Atmos. Chem. Phys.*, 6, 3131-3148, 2006.
- 1263 Andrews, E., Sheridan, P.J., Ogren, J.A., "Seasonal Differences in the Vertical Profiles of
1264 Aerosol Optical Properties over Rural Oklahoma," *Atmos. Chem. Phys.*, 11, 10661–10676,
1265 2011a.
- 1266 Andrews, E., et al. "Climatology of aerosol radiative properties in the free troposphere," *Atmos.*
1267 *Res.*, 102, 365-393, 2011b.
- 1268 Arnott, W.P., Hamasha, K., Moosmuller, H., Sheridan, P.J., Ogren, J.A., "Towards aerosol light-
1269 absorption measurements with a 7-wavelength aethalometer: evaluation with a
1270 photoacoustic instrument and 3-wavelength Nephelometer," *Aerosol Sci. Technol.*, 39, 17-29,
1271 2005.
- 1272 Bahadur, R., Praveen, P. S., Xu, Y., and Ramanathan, V., "Solar absorption by elemental and
1273 brown carbon determined from spectral observations," *P. Natl. Acad. Sci. USA*, 109, 43,
1274 17366–17371, doi:10.1073/pnas.1205910109, 2012.
- 1275 Bergin, M.H., Ogren, J.A., Schwarz, S.E., McInnes, L.M., "Evaporation of Ammonium Nitrate
1276 Aerosol in a Heated Nephelometer: Implications for field measurements," *Environ. Sci.*
1277 *Technol.*, 31, 2878-2883, 1997.
- 1278 Bond, T. C., Anderson, T. L., and Campbell, D., "Calibration and intercomparison of filter-based
1279 measurements of visible light absorption by aerosols," *Aerosol Sci. Technol.*, 30, 582–600,
1280 doi:10.1080/027868299304435, 1999.
- 1281 Bond, T. C., et al., "Bounding the role of black carbon in the climate system: A scientific
1282 assessment," *J. Geophys. Res.*, 118, 5380–5552, doi:10.1002/jgrd.50171, 2013.
- 1283 Bond, T. C., Habib, G., Bergstrom, R.W., "Limitations in the enhancement of visible light
1284 absorption due to mixing state," *J. Geophys. Res.*, 111, D20211, doi:10.1029/2006JD007315,
1285 2006.
- 1286 Brem, B.T., Mena Gonzalez, F.C., Meyers, S.R., Bond, T.C., Rood, M.J., "Laboratory-Measured
1287 Optical Properties of Inorganic and Organic Aerosols at Relative Humidities up to 95%,"
1288 *Aerosol Sci. Technol.*, 46:2, 178-190, 2012.

1289 Buchard, V. da Silva, A.M., Colarco, P.R., Darmenov, A., Randles, C.A., Govindaraju, R.,
1290 Torres, O., Campbell, J., Spurr, R. "Using the OMI aerosol index and absorption aerosol
1291 optical depth to evaluate the NASA MERRA Aerosol Reanalysis," *Atmos. Chem. Phys.*, 15,
1292 5743–5760, 2015.

1293 Burrows, J. P., Dehn, A., Deters, B., Himmelman, S., Richter, A., Voigt, S. and Orphal, J.,
1294 "Atmospheric Remote-Sensing Reference Data from GOME: Part 1. Temperature-
1295 Dependent Absorption Cross-sections of NO₂ in the 231-794 nm Range," *JQSRT*, 60, 1025-
1296 1031, 1998.

1297 Carrico, C.M., Kus, P., Rood, M.J., Quinn, P.K., Bates, T.S., "Mixtures of pollution, dust, sea salt
1298 and volcanic aerosol during ACE-Asia: Radiative properties as a function of relative
1299 humidity," *J. Geophys. Res.*, 108, doi:10.1029/2003JD003405, 2003.

1300 Cappa, C.D., et al., "Radiative absorption enhancements due to the mixing state of atmospheric
1301 black carbon," *Science*, 337, 1078-1081, 2012.

1302 Chin, M., T. Diehl, T., Dubovik, O., Eck, T.F., Holben, B.N., Sinyuk, A., Streets, D.G., "Light
1303 absorption by pollution, dust, and biomass burning aerosols: a global model study and
1304 evaluation with AERONET measurements," *Ann. Geophys.*, 27, 3439-3464, 2009.

1305 Chung, C., Ramanathan, V, Decremer, D., "Observationally constrained estimates of
1306 carbonaceous aerosol radiative forcing," *PNAS*, 109, 11624-11629, 2012.

1307 Corr, C.A., Krotkov, N., Madronich, S., Slusser, J.R., Holben, B., Gao, W., Flynn, J., Lefer, B.,
1308 Kreidenweis, S.M., "Retrieval of aerosol single scattering albedo at ultraviolet wavelengths at
1309 the T1 site during MILAGRO," *Atmos. Chem. Phys*, 9, 5813-5827, 2009.

1310 Corrigan, C.E., Roberts, G.C., Ramana, M.V., Kim, D., Ramanathan, V., "Capturing vertical
1311 profiles of aerosols and black carbon over the Indian Ocean using autonomous unmanned
1312 vehicles," *Atmos. Chem Phys*, 8, 737-747, 2009.

1313 Crumeyrolle, S., Chen, G., Ziemba, L., Beyersdorf, A., Thornhill, L., Winstead, E., Moore, R.,
1314 Shook, M.A., Anderson, B., "Factors that influence surface PM_{2.5} values inferred from
1315 satellite observations: perspective gained for the Baltimore-Washington Area during
1316 DISCOVER-AQ," *Atmos. Chem. Phys.*, 14, 2139-2153, 2014.

1317 Delene, D. J. and Ogren, J. A., "Variability of aerosol optical properties at four North American
1318 surface monitoring sites," *J. Atmos. Sci.*, 59, 1135–1150, 2002.

1319 Doran, J.C., Barnard, J.C., Arnott, W.P., Cary, R., Coulter, R., Fast, J.D., Kassianov, E.I.,
1320 Kleinman, L., Laulainen, N.S., Martin, T., Paredes-Miranda, G., Pekour, M.S., Shaw, W.J.,
1321 Smith, D.F., Springston, S.R., Yu, X.-Y., "The T1-T2 study: evolution of aerosol properties
1322 downwind of Mexico City," *Atmos. Chem. Phys.*, 7, 1585-1598, 2007.

1323 Dubovik, O. and King, M.D., "A flexible inversion algorithm for retrieval of aerosol optical
1324 properties from Sun and sky radiance measurements," *J. Geophys. Res.*, 105, 20673-20696,
1325 2000.

1326 Dubovik, O., Sinyuk, A., Lapyonok, T., Holben, B. N., Mishchenko, M., Yang, P., Eck, T. F.,
1327 Volten, H., Munoz, O., Veihelmann, B., van der Zande, W.J., Leon, J.-F., Sorokin, M.,
1328 Slutsker, I., "Application of spheroid models to account for aerosol particle nonsphericity in
1329 remote sensing of desert dust," *J. Geophys. Res.*, 111, doi:10.1029/2005JD006619, 2006.

1330 Dubovik, O., A. Smirnov, B.N. Holben, M.D. King, Y. J. Kaufman, T.F. Eck and I. Slutsker,
1331 "Accuracy assessment of aerosol optical properties retrieval from AERONET sun and sky
1332 radiance measurements," *J. Geophys. Res.*, 105, 9791-9806, 2000.

1333 Eck, T.F., Holben, B.N., Reid, J.S., Dubovik, O., Smirnov, A., O'Neill, N.T., Slutsker, I. Kinne, S.,
1334 "Wavelength dependence of the optical depth of biomass burning, urban and desert dust
1335 aerosols," *J. Geophys. Res.*, 104, 31 333-31 350, 1999.

1336 Esteve, A.R., Ogren, J.A., Sheridan, P.J., Andrews, E., Holben, B.N., and Utrillas, M.P.,
1337 "Statistical evaluation of aerosol retrievals from AERONET using in-situ aircraft
1338 measurements," *Atmos. Chem. Phys.*, 12, 2987-3003, 2012.

1339 Ferrero, L., Mocnik, G., Ferrini, B.S., Perrone, M.G., Sangiorgi, G., Bolzacchini, E., "Vertical
1340 profiles of aerosol absorption coefficient from micro-aethalometer data and Mie calculation
1341 over Milan," *Sci. Tot. Environ.*, 409, 2824-2837, 2011.

1342 Formenti, P., et al., "STAAARTE-MED 1998 summer airborne measurements over the Aegean
1343 Sea, 2, Aerosol scattering and absorption, and radiative calculations," *J. Geophys. Res.*,
1344 107(D21), 4451, doi:10.1029/2001JD001536, 2002.

1345 Giles, D.M., Holben, B.N., Eck, T.F., Sinyuk, A., Smirnov, A., Slutsker, I., Dickerson, R.R.,
1346 Thompson, A.M., Schafer, J.S., "An analysis of AERONET aerosol absorption properties and
1347 classifications representative of aerosol source region," *J. Geophys. Res.*, 117, doi:
1348 10.1029/2012JD018127, 2012.

1349 Hamonou, E., Chazette, P., Balis, D., Schneider, X., Galani, E., Ancellet, G., Papayannis, A.,
1350 "Characterization of the vertical structure of Saharan dust export to the Mediterranean basin,"
1351 *J. Geophys. Res.*, 104, 22257-22270, 1999.

1352 Hänel, G., "The properties of atmospheric aerosol particles as functions of the relative humidity
1353 at thermodynamic equilibrium with surrounding moist air," *Adv. Geophys.*, 73-188, 1976.

1354 Hansen, J., Sato, M., Ruedy, R., "Radiative forcing and climate response," *J. Geophys. Res.*,
1355 102, 6831-6864, 1997.

1356 Hartley, W.S., Hobbs, P.V., Ross, J.L., Russell, P.B., Livingston, J.M., "Properties of aerosols
1357 aloft relevant to direct aerosol radiative forcing off the mid-Atlantic coast of the United
1358 States," *J. Geophys. Res.*, 105, 9859-9885, 2000.

1359 Haywood, J.M., P. Francis, O. Dubovik, M. Glew, and B. Holben, Comparison of aerosol size
1360 distributions, radiative properties, and optical depths determined by aircraft observations and
1361 Sun photometers during SAFARI 2000, *J. Geophys. Res.*, 108(D13), 8471,
1362 doi:10.1029/2002JD002250, 2003.

1363 Haywood, J.M. and Ramaswamy, V., "Global sensitivity studies of the direct radiative forcing due
1364 to anthropogenic sulfate and black carbon aerosols," *J. Geophys. Res.*, 103, 6043-6058,
1365 1998.

1366 Haywood, J.M. and Shine, K.P., "The effect of anthropogenic sulfate and soot aerosol on the
1367 clear sky planetary radiation budget," *Geophys. Res. Lett.*, 22, 603-606, 1995.

1368 Hinds, W.C., *Aerosol Technology: Properties, behavior and measurement of airborne particles*,
1369 John Wiley and Sons, New York, 1982.

1370 Holben, B. N., et al., "AERONET—A federated instrument network and data archive for aerosol
1371 characterization," *Remote Sens. Environ.*, 66, 1–16, 1998.

1372 Holben, B.N., Eck, T.F., Slutsker, I., Smirnov, A., Sinyuk, A., Schafer, J., Giles, D., Dubovik O.,
1373 "AERONET's Version 2.0 quality assurance criteria,"
1374 http://aeronet.gsfc.nasa.gov/new_web/Documents/AERONETcriteria_final1.pdf, 2006.

1375 Huffman, J.A., Docherty, K.S., Mohr, C., Cubison, M.J., Ulbrich, I.M., Ziemann, P.J., Onasch,
1376 T.B., Jiminez, J.L., "Chemically-resolved volatility measurements of organic aerosol from
1377 different sources," *Environ. Sci. Technol.*, 43, 5351-5357, 2009

1378 Jeong, M.-J. and Li, Z., "Separating real and apparent effects of cloud, humidity, and dynamics
1379 on aerosol optical thickness near cloud edges," *J. Geophys. Res.*, 115,
1380 doi:10.1029/2009JD013547, 2010.

1381 Johnson, B.T., Christopher, S., Haywood, J.M., Osborne, S.R., McFarlane, S., Hsu, C.,
1382 Salustro, C., Kahn, R., "Measurements of aerosol properties from aircraft, satellite and
1383 ground-based remote sensing: A case-study from the Dust and Biomass-burning Experiment
1384 (DABEX)," *Q. J. R. Meteorol. Soc.*, 135, 922–934, 2009.

1385 Johnson, B.T., Osborne, S.R., "Physical and optical properties of mineral dust aerosol
1386 measured by aircraft during the GERBILS campaign," *Q.J.R.Meteorol. Soc.*, 137, 1117-1130,
1387 2011.

1388 Kanaya, Y., Taketani, F., Komazaki, Y., Liu, X., Kondo, Y., Sahu, L., Irie, H., Takashima, H.,
1389 "Comparison of Black Carbon Mass Concentrations Observed by Multi-Angle Absorption

1390 Photometer (MAAP) and Continuous Soot-Monitoring System (COSMOS) on Fukue Island
1391 and in Tokyo, Japan,” *Aerosol Sci. Technol.*, 7:1, 1-10, DOI:
1392 10.1080/02786826.2012.716551, 2013.

1393 Kasten, F., “Visibility forecast in the phase of pre-condensation,” *Tellus*, 21, 631-635, 1969.

1394 Kelecksoglou, K., Rapsomanikis, S., Karageorgos, E.T., Kosmadakis, I., Optical properties of
1395 aerosol over a Southern European urban environment,” *Int.J. Remote Sens.*, 33, 1214-1233,
1396 2012.

1397 Kinne et al., “An AeroCom initial assessment – optical properties in aerosol component modules
1398 of global models,” *Atmos. Chem. Phys.*, 6, 1–20, 2006.

1399 Koch, D., et al., “Evaluation of black carbon estimations in global aerosol models,” *Atmos.Chem.*
1400 *Phys.*, 9, 9001–9026, doi:10.5194/acp-9-9001-2009, 2009.

1401 Kotchenruther, R. A., Hobbs, P.V., Hegg, D.A., “Humidification factors for atmospheric aerosols
1402 off the mid-Atlantic coast of the United States,” *J. Geophys. Res.*, 104, 2239– 2251, 1999.

1403 Lacagnina, C., Hasekamp, O.P., Bian, H., Curci, G., Myhre, G., van Noije, T, Schulz, M., Skeie,
1404 R.B., Takemura, T., Zhang, K., “Aerosol single-scattering albedo over the global oceans:
1405 Comparing PARASOL retrievals with AERONET, OMI, and AeroCom models estimates,” *J.*
1406 *Geophys. Res. Atmos.*, 120, 9814–9836, doi:10.1002/2015JD023501, 2015.

1407 Lack, D.A., et al., “Relative humidity dependence of light absorption by mineral dust after long-
1408 range atmospheric transport from the Sahara,” *Geophys. Res. Lett.*, 36, L24805,
1409 doi:10.1029/2009GL041002, 2009.

1410 Lack, D.A., Cappa, C.D., Covert, D.S., Baynard, T., Massoli, P., Sierau, B., Bates, T.S., Quinn,
1411 P.K., Lovejoy, E.R., Ravishankara, A.R., “Bias in Filter-Based Aerosol Light Absorption
1412 Measurements Due to Organic Aerosol Loading: Evidence from Ambient Measurement,”
1413 *Aerosol Sci. and Technol.*, 42, 1033–1041, 2008.

1414 Lack, D.A., Richardson, M.S., Law, D., Langridge, J.M., Cappa, C.D., McLaughlin, R.J., and
1415 Murphy, D.M.: Aircraft Instrument for Comprehensive Characterization of Aerosol Optical
1416 Properties, Part 2: Black and Brown Carbon Absorption and Absorption Enhancement
1417 Measured with Photo Acoustic Spectroscopy, *Aerosol Sci. Tech.*, 46:5, 555-568, DOI:
1418 10.1080/02786826.2011.645955, 2012.

1419 Leahy, L.V., Anderson, T.L., Eck, T.F., Bergstrom, R.W., “A synthesis of single scattering
1420 albedo of biomass burning aerosol over southern Africa during SAFARI 2000,” *Geophys.*
1421 *Res. Lett.*, 34, doi:10.1029/2007GL029697, 2007.

1422 Li, S., Kahn, R., Chin, M., Garay, M.J., Liu, Y., “Improving satellite-retrieved aerosol
1423 microphysical properties using GOCART data,” *Atmos. Meas. Tech.*, 8, 1157–1171, 2015.

1424 Ma, X. and Yu, F., “Seasonal variability of aerosol vertical profiles over east US and west
1425 Europe: GEOS-Chem/APM simulation and comparison with CALIPSO observations,” *Atmos.*
1426 *Res.*, 140-141, 28-37, ttp://dx.doi.org/10.1016/j.atmosres.2014.01.001, 2014.

1427 Magi, B.I., Hobbs, P.V., Kirchstetter, T.W., Novakov, T., Hegg, D.A., Gao, S., Redemann, J.,
1428 Schmid, B., “Aerosol Properties and Chemical Apportionment of Aerosol Optical Depth at
1429 Locations off the U.S. East Coast in July and August 2001,” *J. Atmos. Sci.*, 62, 919-933,
1430 2005.

1431 Magi, B.I., Hobbs, P.V., Schmid, B., Redemann, J., “Vertical profiles of light scattering, light
1432 absorption and single scattering albedo during the dry biomass burning season in southern
1433 Africa and comparisons of in-situ and remote sensing measurements of aerosol optical
1434 depths,” *J. Geophys. Res.*, 108, doi:10.1029/2002JD00236, 2003

1435 Mallet, M., Dubovik, O., Nabat, P., Dulac, F., Kahn, R., Sciare, J., Paronis, D., and Léon, J. F.,
1436 “Absorption properties of Mediterranean aerosols obtained from multi-year, ground-based
1437 remote sensing observations,” *Atmos. Chem. Phys.*, 13, 9195-9210, 2013.

1438 Mallet, M., Van Dingenen, R., Roger, J. C., Despiiau, S., Cachier, H., "In situ airborne
1439 measurements of aerosol optical properties during photochemical pollution events," J.
1440 Geophys. Res., 110, D03205, doi:10.1029/2004JD005139, 2005.

1441 Mallet, M., Pont, V., Liousse, C., Gomes, L., Pelon, J., Osborne, S., Haywood, J., Roger, J.C.,
1442 Dubuisson, P., Mariscal, A., Thouret, V., Gouloub, P., "Aerosol direct radiative forcing of
1443 Djougou (northern Benin) during the African Monsoon Multidisciplinary, Analysis dry season
1444 experiment (special observation period – 0)," J. Geophys. Res., 113,
1445 doi:1029/2007JD009419, 2008.

1446 Malm, W.C., Sisler, J.F., Huffman, D., Eldred, R.A., Cahill, T.A., "Spatial and seasonal trends in
1447 particle concentration and optical extinction in the United States," J. Geophys. Res. 99,
1448 1347–1370, 1994.

1449 McConnell, C.L., Highwood, E.J., Coe, H., Formenti, P., Anderson, B., Osborne, S., Nava, S.
1450 Desboeufs, K., Chen, G., and Harrison, M.A.J., "Seasonal variations of the physical and
1451 optical characteristics of Saharan dust: Results from the Dust Outflow and Deposition to the
1452 Ocean (DODO) experiment," J. Geophys. Res., 113, doi:10.1029/2007JD009606, 2008.

1453 McMeeking, G. R., Fortner, E., Onasch, T.B., Taylor, J.W., Flynn, M., Coe, H., Kreidenweis,
1454 S.M. "Impacts of nonrefractory material on light absorption by aerosols emitted from biomass
1455 burning," J. Geophys. Res. Atmos., 119, 12,272–12,286, doi:10.1002/2014JD021750, 2014.

1456 Mendes, L., Eleftheriadis, K., Biskos, G., "Performance comparison of two thermal denuders in
1457 volatility tandem DMA measurements," J. Aerosol Sci., 92, 38-52, 2016.

1458 Müller, D., Lee, K.-H., Gasteiger, J., Tesche, M., Weinzierl, B., Kandler, K., Müller, T., Toledano,
1459 C., Otto, S., Althausen, D., Ansmann, A., "Comparison of optical and microphysical
1460 properties of pure Saharan mineral dust observed with AERONET Sun photometer, Raman
1461 lidar, and in situ instruments during SAMUM 2006," J. Geophys. Res., 117, doi:
1462 10.1029/2011JD016825, 2012.

1463 Müller, T., et al. "Characterization and intercomparison of aerosol absorption photometers:
1464 result of two intercomparison workshops" Atmos. Meas. Tech., 4, 245–268, 2011.

1465 Myhre G., Samset, B.H., Schulz, M. et al., "Radiative forcing of the direct aerosol effect from
1466 AeroCom Phase II simulations," Atmos. Chem. Phys., 13, 1853–1877, 2013

1467 Nessler, R., Weingartner, E., Baltensperger, U., "Effect of humidity on aerosol light absorption
1468 and its implications for extinction and the single scattering albedo illustrated for a site in the
1469 lower free troposphere," J. Aerosol Sci., 36, 958–972, 2005.

1470 Ogren, J. A., "Comment on "Calibration and Intercomparison of Filter-Based Measurements of
1471 Visible Light Absorption by Aerosols", Aerosol Sci. Technol., 44, 589–591,
1472 doi:10.1080/02786826.2010.482111, 2010.

1473 O'Neill, N. T., Eck, T. F., Smirnov, A., Holben, B. N., Thulasiraman, S., "Spectral discrimination
1474 of coarse and fine mode optical depth," J. Geophys. Res., 108, 4559-4573, 2003.

1475 Osborne, S. R., Johnson, B. T., Haywood, J. M., Baran, A. J., Harrison, M. A. J., McConnell,
1476 C.L., "Physical and optical properties of mineral dust aerosol during the Dust and Biomass-
1477 burning Experiment, J. Geophys. Res., 113, D00C03, doi:10.1029/2007JD009551, 2008.

1478 Pan, X., Chin, M., Gautam, R., Bian, H., Kim, D., Colarco, P.R., Diehl, T.L., Takemura, T.,
1479 Pozzoli, L., Tsigaridis, K., Bauer, S., Bellouin, N., "A multi-model evaluation of aerosols over
1480 South Asia: common problems and possible causes," Atmos. Chem. Phys., 15, 5903–5928,
1481 2015.

1482 Parworth, C., Fast, J., Meib, F., Shipper, T., Sivaraman, C., Tilp, A., Watson, T., Zhang, Q.,
1483 "Long-term measurements of submicrometer aerosol chemistry at the Southern Great Plains
1484 (SGP) using an Aerosol Chemical Speciation Monitor (ACSM)," Atmos. Environ., 106, 43–55,
1485 2015.

1486 Petzold, A., Ogren, J.A., Fiebig, M., Laj, P., Li, S.-M., Baltensperger, U., Holzer-Popp, T., Kinne,
1487 S., Pappalardo, G., Sugimoto, N., Wehrli, C., Wiedensohler, A., Zhang, X.-Y.,

1488 “Recommendations for reporting “black carbon” measurements,” *Atmos. Chem. Phys.*, 13,
1489 8365-8379, 2013.

1490 Quinn, P.K., Bates, T.S., Baynard, T., Clarke, A.D., Onasch, T.B., Wang, W., Rood, M.J.,
1491 Andrews, E., Allan, J., Carrico, C.M., Coffman, D., Worsnop, D., “Impact of particulate
1492 organic matter on the relative humidity dependence of light scattering: A simplified
1493 parameterization,” *Geophys. Res. Lett.*, 32, doi:10.1029/2005GL024322, 2005.

1494 Ramanathan, V., Carmichael, G., “Global and regional climate changes due to black carbon,”
1495 *Nature – Geosci.*, 1(4), 221-227, 2008.

1496 Reddy, M. S., Boucher, O. Bellouin, N., Schulz, M., Balkanski, Y., Dufresne, J.L., Pham, M.,
1497 “Estimates of global multicomponent aerosol optical depth and direct radiative perturbation in
1498 the Laboratoire de Meteorologie Dynamique general circulation model,” *J. Geophys. Res.*,
1499 110, doi:10.1029/2004jd004757, 2005.

1500 Redemann, J., Russell, P.B., Hamill, P., “.,” “Dependence of aerosol light absorption and single
1501 scattering albedo on ambient relative humidity for sulfate aerosols with black carbon cores,”
1502 *J. Geophys. Res.*, 106, 27485-27495, 2001.

1503 Reid, J.S., Hobbs, P.V., Liousse, C., Vanderlei Martins, J., Weiss, R.E., Eck, T.F.,
1504 “Comparisons of techniques for measuring shortwave absorption and black carbon content of
1505 aerosols from biomass burning in Brazil,” *J. Geophys. Res.*, 103, 32031-32040, 1998.

1506 Samset, B.H. et al., “Black carbon vertical profiles strongly affect its radiative forcing
1507 uncertainty,” *Atmos. Chem. Phys.*, 13, 2423–2434, 2013.

1508 Sato, M., Hansen, J., Kock, D., Lacis, A., Ruedy, R., Dubovik, O., Holben, B., Chin, M.,
1509 Novakov, T., “Global atmospheric black carbon inferred from AERONET,” *PNAS*, 100, 6319-
1510 6324, 2003.

1511 Schafer, J.S., Eck, T.F., Holben, B.N., Thornhill, K.L., Anderson, B.E., Sinyuk, A., Giles, D.M.,
1512 Winstead, E.L., Ziemba, L.D., Beyersdorf, A.J., Kenny, P.R., Smirnov, A., Slutsker, I.,
1513 “Intercomparison of aerosol single-scattering albedo derived from AERONET surface
1514 radiometers and LARGE in situ aircraft profiles during the 2011 DRAGON-MD and
1515 DISCOVER-AQ experiments,” *J. Geophys. Res.*, 119, 7439–7452,
1516 doi:10.1002/2013JD021166, 2014.

1517 Schmid, B., Flynn, C.J., Newsom, R.K., Turner, D.D., Ferrare, R.A., Clayton, M.F., Andrews, E.,
1518 Ogren, J.A., Johnson, R.R., Russell, P.B., Gore, W.J., Dominguez, R., “Validation of aerosol
1519 extinction and water vapor profiles from routine Atmospheric Radiation Measurement
1520 Program Climate Research Facility measurements,” *J. Geophys. Res.*, 114,
1521 doi:10.1029/2009JD012682, 2009.

1522 Schutgens, N.A.J., Partridge, D.G., Stier, P., “The importance of temporal collocation for the
1523 evaluation of aerosol models with observations,” *Atmos. Chem. Phys.*, 16, 1065–1079, 2016.

1524 Schwarz, J.P., Spackman, J.R., Fahey, D.W., Gao, R.W., Lohmann, U., Stier, P., Watts, L.A.,
1525 Thomson, D.S., Lack, D.A., Pfister, L., Mahoney, M.J., Baumgardner, D., Wilson, J.C.,
1526 Reeves, J.M., “Coatings and their enhancement of black carbon light absorption in the
1527 tropical atmosphere,” *J. Geophys. Res.*, 113, D03203, doi:10.1029/2007JD009042, 2008.

1528 Schwarz, J.P., Spackman, J.R., Gao, R.S., Watts, L.A., Stier, P., Schulz, M., Davis, S.M.,
1529 Wofsy, S.C., Fahey, D.W., “Global-scale black carbon profiles observed in the remote
1530 atmosphere and compared to models,” *Geophys. Res. Lett.*, 27, doi:10.1029/2010GL044372,
1531 2010.

1532 Sharma, S., Ishizawa, M., Chan, D., Lavoue, D., Andrews, E., Eleftheriadis, K, Maksyutov, S.,
1533 “16-year simulation of Arctic black carbon: transport, source contribution, and sensitivity
1534 analysis on deposition,” *J. Geophys. Res.* 118, 1–22, doi:10.1029/2012JD017774, 2013.

1535 Sheridan, P. J., Andrews, E., Ogren, J. A., Tackett, J. L., and Winker, D. M.: Vertical profiles of
1536 aerosol optical properties over Central Illinois and comparison with surface and satellite
1537 measurements, *Atmos. Chem. Phys.*, 12, 11695-11721, 2012.

1538 Sheridan, P. J., Arnott, W. P., Ogren, J. A., Andrews, E., Atkinson, D. B., Covert, D. S.,
 1539 Moosmüller, H., Petzold, A., Schmid, B., Strawa, A. W., Varma, R., and Virkkula, A.: The
 1540 Reno Aerosol Optics Study: An Evaluation of Aerosol Absorption Measurement Methods,
 1541 *Aerosol Sci. Tech.*, 39, 1–16, 2005.
 1542 Sheridan, P. J., Delene, D. J., Ogren, J.A., “Four years of continuous surface aerosol
 1543 measurements from the Department of Energy’s Atmospheric Radiation Measurement
 1544 Program Southern Great Plains Cloud and Radiation Testbed site,” *J. Geophys. Res.*, 106,
 1545 20735–20747, 2001.
 1546 Sheridan, P.J., Jefferson, A., Ogren, J.A., “Spatial variability of submicrometer aerosol radiative
 1547 properties over the Indian Ocean during INDOEX,” *J. Geophys. Res.*, 107, D19, 8011,
 1548 10.1029/2000JD000166, 2002.
 1549 Sherman, J. P., Sheridan, P. J., Ogren, J. A., Andrews, E., Hageman, D., Schmeisser, L.,
 1550 Jefferson, A., and Sharma, S.: A multi-year study of lower tropospheric aerosol variability and
 1551 systematic relationships from four North American regions, *Atmos. Chem. Phys.*, 15, 12487-
 1552 12517, doi:10.5194/acp-15-12487-2015, 2015.
 1553 Shinozuka, Y., Redemann, J., Livingston, J. M., Russell, P. B., Clarke, A. D., Howell, S. G.,
 1554 Freitag, S., O’Neill, N. T., Reid, E. A., Johnson, R., Ramachandran, S., McNaughton, C. S.,
 1555 Kapustin, V. N., Brekhovskikh, V., Holben, B. N., and McArthur, L. J. B.: Airborne observation
 1556 of aerosol optical depth during ARCTAS: vertical profiles, inter-comparison and fine-mode
 1557 fraction, *Atmos. Chem. Phys.*, 11, 3673–3688, 2011.
 1558 Sinha, P., Hobbs, P.V., Yokelson, R.J., Bertschi, I.T., Blake, D.R., Simpson, I., Gao, S.,
 1559 Kirchstetter, T.W., Novakov, T., “Emissions of trace gases and particles from savanna fires in
 1560 southern Africa,” *J. Geophys. Res.*, 108, 8487, doi:10.1029/2002JD002325, 2003.
 1561 Sinha, P.R., Kondo, Y., Koike, M., Ogren, J.A., Jefferson, A., Barrett, T.E., Sheesley, R.J.,
 1562 Ohata, S., Moteki, N., Coe, H., Liu, D., Irwin, M., Tunved, P., Quinn, P.K., Zhao, Y.,
 1563 “Evaluation of ground-based black carbon measurements by filter-based photometers at two
 1564 Arctic sites,” in revisions for *J. Geophys. Res.*, 2017.
 1565 Skeie, R. B., T. Berntsen, G. Myhre, C. A. Pedersen, J. Ström, S. Gerland, and J. A. Ogren,
 1566 “Black carbon in the atmosphere and snow, from pre-industrial times until present,” *Atmos.*
 1567 *Chem. Phys.*, 11, 6809-6836, doi:10.5194/acp-11-6809-2011, 2011.
 1568 Smirnov, A., B. N. Holben, T. F. Eck, O. Dubovik, and I. Slutsker, “Cloud screening and quality
 1569 control algorithms for the AERONET database,” *Remote Sens. Environ.*, 73, 337– 349, 2000.
 1570 Subramanian, R., Roden, C. A., Boparai, P., and Bond, T. C.: Yellow beads and missing
 1571 particles: Trouble ahead for filter-based absorption measurements, *Aerosol Sci. Technol.*,
 1572 41(6), 630–637, DOI: 10.1080/02786820701344589, 2007.
 1573 Taubman, B.F., Hains, J.C., Thompson, A.M., Marufu, L.T., Doddridge, B.G., Stehr, J.W., Piety,
 1574 C.A., and Dickerson, R.R., “Aircraft vertical profiles of trace gas and aerosol pollution over
 1575 the mid-Atlantic United States: Statistics and meteorological cluster analysis,” *J. Geophys.*
 1576 *Res.*, 111, D10S07, doi:10.1029/2005JD006196, 2006.
 1577 Turner, D.D., Ferrare, R.A., Brasseur, L.A., “Average Aerosol Extinction and Water Vapor
 1578 Profiles over the Southern Great Plains,” *Geophys. Res. Lett.*, 28, 4441-4444,
 1579 Vaden, T.D., Imre, D., Baranek, J., Shrivastava, M., Zelenyuk, A., Finlayson-Pitts, B.J.,
 1580 “Evaporation kinetics and phase of laboratory and ambient secondary organic aerosol,”
 1581 *PNAS*, 108, 2190-2195, 2011.
 1582 Virkkula, A.: Correction of the Calibration of the 3-wavelength Particle Soot Absorption
 1583 Photometer (3 PSAP), *Aerosol Sci. Technol.*, 44, 706–712, 2010.
 1584 Wang, R., et al., “Estimation of global black carbon direct radiative forcing and its uncertainty
 1585 constrained by observations,” *J. Geophys. Res. Atmos.*, 121, 5948–5971,
 1586 doi:10.1002/2015JD024326, 2016.
 1587 Wang, X., Heald, C.L., Ridley, D.A., Schwarz, J.P., Spackman, J.R., Perring, A.E., Coe, H., Liu,
 1588 D., Clarke, A.D., “Exploiting simultaneous observational constraints on mass and absorption

1589 to estimate the global direct radiative forcing of black carbon and brown carbon,” *Atmos.*
1590 *Chem. Phys.*, 14, 10989–11010, 2014.
1591 Yu, F., Chin, M., Winker, D.M., Omar, A. H., Liu, Z., Kittaka, C., Diehl, T., “Global view of
1592 aerosol vertical distributions from CALIPSO lidar measurements and GOCART simulations:
1593 Regional and seasonal variations,” *J. Geophys. Res.*, 115, D00H30,
1594 doi:10.1029/2009JD013364, 2010.
1595
1596

1597 **Tables**

1598

1599

1600

1601

1602 **Table 1a** Statistical values (medians, means and standard deviations) of AERONET versus in-
 1603 situ comparison where there was an AERONET retrieval within +/-3 h of the end of a 2 h flight
 1604 profile. AERONET values are for Level-1.5 data when there was a Level-2 AOD value and an
 1605 almucantar retrieval. (First value in each cell is median; second set of values in each cell are
 1606 mean± Std.Dev, third row is number of AERONET retrievals corresponding to flights (in
 1607 AERONET columns) or number of flights (In-situ columns)). These numbers represent the blue
 1608 points in Figures 3-5.

	BND		SGP	
	AERONET	In-situ	AERONET	In-situ
AOD	0.118; 0.146±0.099	0.114; 0.135±0.139	0.138; 0.146±0.099	0.137; 0.147±0.077
AAOD	0.013; 0.013±0.007	0.003; 0.005±0.006	0.019; 0.023±0.008	0.004; 0.004±0.003
SSA	0.895; 0.898±0.034	0.961; 0.964±0.020	0.847; 0.839±0.038	0.971; 0.973±0.011
#	51 retrievals ¹	21 flights	23 retrievals ¹	11 flights

1609 ¹retrievals are flight-averaged prior to calculating statistics.

1610

1611 **Table 1b** Statistical values (medians, means and standard deviations) of AERONET versus in-
 1612 situ comparison where there was an AERONET retrieval within +/-3 h of the end of a 2 h flight
 1613 profile and AERONET AOD₄₄₀>0.2. AERONET values are for Level-1.5 data when there was a
 1614 Level-2 AOD value and an almucantar retrieval. (First value in each cell is median; second set
 1615 of values in each cell are mean± Std.Dev, third row is number of AERONET retrievals
 1616 corresponding to flights (in AERONET columns) or number of flights (In-situ columns)). These
 1617 numbers represent the purple points in Figures 4-5.

	BND		SGP	
	AERONET	In-situ	AERONET	In-situ
AOD	0.306; 0.304±0.125	0.299; 0.331±0.230	0.269	0.238
AAOD	0.025; 0.019±0.012	0.010; 0.013±0.012	0.034	0.009
SSA	0.941; 0.942±0.023	0.971; 0.966±0.010	0.875	0.964
#	6 retrievals ¹	4 flights	2 retrievals	1 flights

1618 ¹retrievals are flight-averaged prior to calculating statistics.

1619

1620

1621

1622

1623
1624
1625
1626
1627
1628
1629
1630
1631
1632
1633
1634
1635
1636

Table 2 Number of AERONET/IN-SITU AOD and AAOD flight matches as a function of various AERONET constraints and the +/- 3h time window.

	BND (2006-2009)	SGP(2005-2007)
Total profile flights	402	171
Level-2 AOD	73	37
Level-2 AOD+almucantar retrieval ¹	21	11
Level-2 AOD+almucantar retrieval+AOD ₄₄₀ >0.20	2	1
Level-1.5* AAOD	21	11
Level-1.5* AAOD + AOD ₄₄₀ >0.20	4	1
Level-2 AAOD	1	0

¹an almucantar retrieval does not necessarily imply an AAOD retrieval

Table 3 Direct AOD comparisons – AERONET ("RS") vs In-Situ ("IS")

Study, # profiles Citation(s)	Location, aerosol type AOD comments Alt. range	Instruments corrections size cut	AAOD comparison information	Comments
BND 24 profiles This study	Central US Rural, continental AOD ₄₄₀ range: 0.04-0.55 AOD comparison See Fig. 3a 150-4200 m agl	PSAP-3wave TSI neph-3wave B1999, O2010, AO1998 f(RH) adjust Dp<5-7 μm	Wavelength=440, 670 nm Ångström interpolation RS AAOD>IS AAOD AAOD ₄₄₀ range: 0.001-0.042	Profiles matched within 3 hours of AERONET measurement. Profiles within 15 km of AERONET measurement. Used V2 AERONET Level 1.5 AAOD values for cases with valid V2 AERONET Level 2.0 AOD value. Extrapolated from lowest altitude range to ground to account for aerosol below plane
SGP 14 profiles This study	Central US Rural, continental AOD ₄₄₀ range: 0.06-0.43 AOD comparison See Fig. 3b 150-4200 m agl	PSAP-3wave TSI neph-3wave B1999, O2010, AO1998 f(RH) adjust Dp<5-7 μm	Wavelength=440, 670 nm Ångström interpolation RS AAOD>IS AAOD AAOD ₄₄₀ range: 0.012-0.052	Profiles matched within 3 hours of AERONET measurement. Profiles within 1 km of AERONET measurement Used V2 AERONET Level 1.5 AAOD values for cases with valid V2 AERONET Level 2.0 AOD value. Extrapolated from lowest altitude range to ground to account for aerosol below plane
MAC 13 profiles Corrigan et al., 2008	Indian Ocean Pollution AOD ₄₄₀ range: 0.1-0.6	Aethalometer 3-wave OPC +Mie for scattering A2005	Wavelength not provided RS AAOD>IS AAOD AAOD ₄₄₀ range: 0.005-0.033	No details on how profiles matched with retrievals in terms of time or distance. No details on version of AERONET data used; this is relevant, given low AODs in first half of study – not sure if there were comparisons for low AODs.

	No AOD comparison 0-3200 m asl	Dp<5 μm		Note: this study is the one cited by Bond et al. (2013) to support the use of AERONET to scale modeled BC values
--	-----------------------------------	---------	--	--

In-situ instrument corrections: B1999=Bond et al., 1999; O2010=Ogren, 2010, AO1998=Anderson and Ogren, 1998; A2005=Arnott et al., 2005; Ångström interpolation – indicates in-situ wavelength adjusted to AERONET wavelength using Ångström interpolation; f(RH) adjust – indicates the in-situ measurements were adjusted to ambient humidity conditions for the AOD comparison. IS=In-situ measurements, RS=Remote sensing (AERONET) measurements

Table 4 SSA comparisons – AERONET vs In-situ

Study, # profiles Citation(s)	Location, aerosol type AOD comments Alt. range	Instruments, Corrections, Inlet size cut	SSA comparison information	Comments
BND 24 profiles This study	Central US Rural, continental AOD ₄₄₀ range: 0.04-0.55 AOD comparison: See Fig. 2a 150-4200 m agl	PSAP-3wave TSI neph-3wave B1999, O2010, AO1998 f(RH) adjust Dp<5-7 μm	Wavelength=440, 670 nm Ångström interpolation RS SSA<IS SSA	Profiles matched within 3 hours of AERONET measurement. Profiles within 15 km of AERONET measurement. Used V2 AERONET Level 1.5 AAOD values for cases with valid V2 AERONET Level 2.0 AOD value. Extrapolated from lowest altitude range to ground to account for aerosol below plane
SGP 14 profiles This study	Central US Rural, continental AOD ₄₄₀ range: 0.06-0.43 AOD comparison:	PSAP-3wave TSI neph-3wave B1999, O2010, AO1998 f(RH) adjust	Wavelength=440, 670 nm Ångström interpolation RS SSA<IS SSA	Profiles matched within 3 hours of AERONET measurement. Profiles within 1 km of AERONET measurement. Used V2 AERONET Level 1.5 AAOD values for cases with valid V2 AERONET Level 2.0 AOD value.

	See Fig. 2b 150-4200 m agl	Dp<5-7 μm		Extrapolated from lowest altitude range to ground to account for aerosol below plane
AAO (BND) 1 profile Esteve et al., 2012	Central US Rural, continental AOD ₅₅₀ = 0.65 AOD comparison: RS AOD>IS AOD 150-4200 m agll	PSAP-3wave TSI neph-3wave B1999, O2010, AO1998 f(RH) adjust Dp<5-7 μm	Wavelength=550 nm Power law interpolation RS SSA < IS SSA	Profiles matched within 2 hours of AERONET measurement. Profiles within 15 km of AERONET measurement. Used V2 AERONET Level 2.0 AOD value. Extrapolated from lowest altitude range to ground to account for aerosol below plane
DISCOVER-AQ 12 profiles Schafer et al., 2014	East Coast US Polluted air AOD ₄₄₀ >0.2 AOD compare: RS AOD > IS AOD (by 23%)* 367-3339 m	PSAP-3wave TSI neph-3wave V2010, AO1998* f(RH) adjust Dp<4 μm *	Wavelength=550 nm AERONET "interpolated" to 550 (no detail provided) In-situ absorption interpolated to 550 using Ångström interpolation RS SSA < IS SSA	Profile matched within 45 min of AERONET measurement. Profile within 1 km of AERONET measurement. Used V2 AERONET Level 2.0 values in paper Altitude range: at least <500 m and >1500 m for column comparisons, min and max altitudes: 367 m and 3339 m Did not specify agl or asl but those are similar for the location.
CLAMS 1 profile Magi et al., 2005	East Coast US Polluted air AOD ₄₄₀ =0.60 AOD comparison: RS AOD > IS AOD (by 15%)	PSAP-1wave MSE neph-3wave B1999, AO1998 f(RH) adjust Inlet size cut not reported, Sinha,	Wavelength=550 nm Wave_adj =quadratic polynomial interpolation RS SSA < IS SSA	Profile matched within 1 hour of AERONET measurement. Profile within 3 km of AERONET measurement. Retrieved V2 AERONET Level 2.0 AOD ₄₄₀ from http://aeronet.gsfc.nasa.gov/ Also compared campaign AERONET average

	170-1500 m agl	2003 suggests Dp<4 μm		with profile average: SSA's much closer, but profiles weren't necessarily close in time or space to AERONET site
ESCOMPTE 1 profile Mallet et al., 2005	Avignon, France Pollution AOD ₄₄₀ >0.55 No AOD comparison 100-2900 m	PSAP-1wave TSI neph-3wave B1999, A1999 No f(RH) adj Inlet Dp not given	Wavelength=550 nm Wave_adj = estimated from visual inspection (spectral dependence is relatively flat) RS SSA < IS SSA	Profile matched within 1 hour of AERONET measurement. Profile within 10 km of AERONET measurement. Used V2 AERONET Level 2.0 AOD ₄₄₀ from http://aeronet.gsfc.nasa.gov/ , not stated in paper. Did not adjust in-situ measurements for f(RH), so presumably IS SSA would increase so it was even larger than RS SSA. Did not specify agl or asl
SAFARI 5 profiles Leahy et al., 2007 UW plane	Southern Africa Biomass burning AOD ₅₅₀ >0.28-1.12 AOD comparison: RS AOD > IS AOD RS=1.12*IS-0.05 R ² =0.99 100-5320 m asl	PSAP-1wave MSE neph-3wave B1999;H2000 f(RH) adjust Dp<4 um	Wavelength=550 nm Wave_adj= 2nd order polynomial For AOD ₅₅₀ >0.6 (3 profiles) RS SSA > IS SSA For AOD ₅₅₀ <0.3 (2 profiles) RS SSA ≤ IS SSA	Profiles matched within 1-4 hours of AERONET measurement. Profiles within 20 km of AERONET measurement. Used V2 AERONETLevel 2.0 Also found: AEROCOM model>insitu Altitude range is min and max over 5 flights – no flights covered that entire range). They used AATS to account for aerosol above plane and extrapolated down to acct for aerosol below plane. (Altitude range from flight info in Magi et al., 2003)

<p>SAFARI 1 profile</p> <p>Haywood et al, 2003 C-130</p>	<p>Southern Africa Biomass burning</p> <p>AOD₄₄₀=0.71</p> <p>AOD comparison: RS AOD < IS AOD</p> <p>330-3420 m agl</p>	<p>PSAP-1wave TSI neph-3wave</p> <p>B1999,AO1998 No f(RH) adj</p> <p>Dp<2-4 μm</p>	<p>Wavelength=native Wave_adj = none</p> <p>RS SSA < IS SSA</p>	<p>Profile matched within 2 hours of AERONET measurement. Profiles within 10 km of AERONET measurement.</p> <p>Used V2 AERONET Level 2.0 data from http://aeronet.gsfc.nasa.gov/</p> <p>They defend the lack of f(RH) correction because (a) ambient RH values < 56% and (b) previous measurements of f(RH) of BB aerosol suggest minimal hygroscopicity</p> <p>Paper mostly focused on size dist comparison; SSA comparison seems like afterthought.</p> <p>Extrapolated from lowest altitude range to ground to account for aerosol below plane</p>
<p>DABEX 3 profiles</p> <p>Osborne et al., 2008</p>	<p>Africa Dust/BB</p> <p>AOD comparison RS AOD < IS AOD (by up to 40%)</p> <p>AOD₅₅₀~0.3-0.6</p> <p>100-5000 m</p>	<p>PSAP-1wave TSI neph-3wave</p> <p>B1999,AO1998 No f(RH) adj</p> <p>Dp<2-4 μm</p>	<p>Wavelength=550 nm Wave_adj=log interpolation</p> <p>RS SSA < IS SSA</p>	<p>No details on how profiles matched with retrievals in terms of time. Profiles within 100 km of AERONET measurement</p> <p>Used V2 AERONET Level 2.0</p> <p>They defend the lack of f(RH) correction because (a) ambient RH values are mostly low (<60%) and (b) previous measurements of f(RH) of BB aerosol suggest minimal hygroscopicity</p> <p>Jan 21, 23 and 30 profiles IS overpredicts AOD so IS SSA is greater</p>

				<p>than RS SSA</p> <p>Suggest it could be due to large particle correction to IS measurements using PCASP. McConnell et al., (2008) suggests problems with nephelometer sensitivity</p> <p>Did not specify agl or asl Altitude range is min and max over 4 flights – no flights covered that entire range</p>
<p>DABEX 1 profile</p> <p>Johnson et al., 2009</p>	<p>Africa DUST/BB</p> <p>AOD comparison: RS AOD < IS AOD (by ~10%)</p> <p>AOD₅₅₀ > 0.7</p> <p>150-3000 m</p>	<p>PSAP-1wave TSI neph-3wave</p> <p>B1999,AO1998 No f(RH) adj</p> <p>Dp<2-4 μm</p>	<p>Wavelength=550 nm Wave_adj=log interpolation</p> <p>RS SSA < IS SSA</p>	<p>Profile matched within 1 hour of AERONET measurement. Profile within 100 km of AERONET measurement</p> <p>Used V2 AERONET Level 2.0</p> <p>They defend the lack of f(RH) correction because ambient RH values are mostly low (<40% with a max of 70%)</p> <p>Jan 19 profile</p> <p>Incorrectly used Mie to adjust σ_{ap} to 550 after B1999 applied</p> <p>Did not specify agl or asl</p>

IS=In-situ measurements, RS=Remote sensing (AERONET) measurements. In-situ instrument corrections: B1999=Bond et al., 1999; V2010=Virkula et al., 2010;O2010=Ogren, 2010; AO1998=Anderson and Ogren, 1998; H2000=Hartley et al., 2000; A2005=Arnott et al., 2005; Ångström interpolation – indicates wavelength adjustment using Ångström exponent interpolation; f(RH) adjust – indicates the in-situ measurements were adjusted to ambient humidity conditions for the AOD and SSA comparison.
*Information about Discover-AQ flights from Crumreylle et al. (2014)

Figures

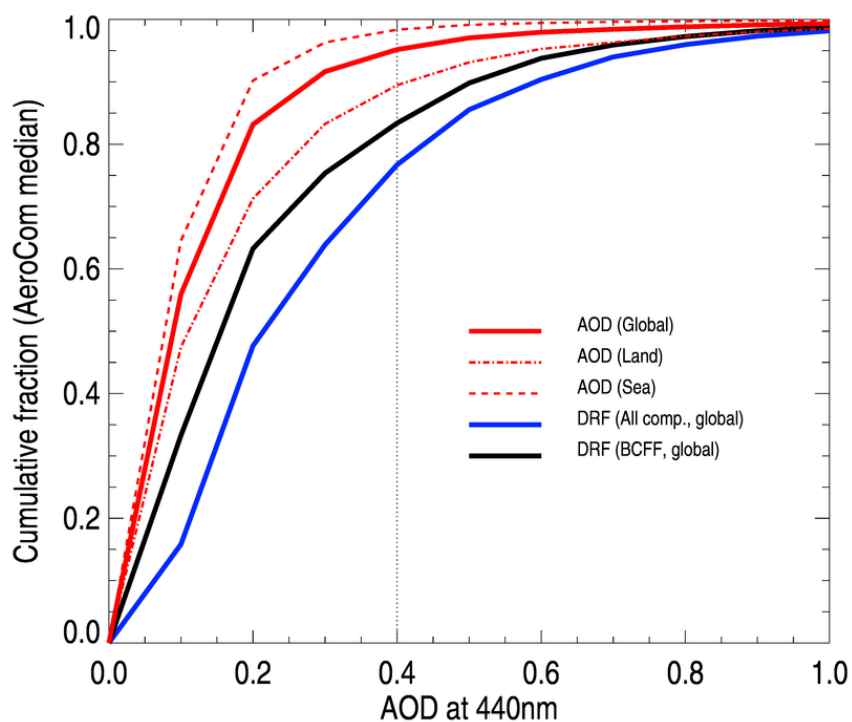


Figure 1. Cumulative AOD_{440} frequency distribution (red lines) based on output from five AeroCom models. Blue and black lines show contribution of total aerosol and fossil fuel black carbon, respectively, to the global radiation budget as a function of AOD_{440} . See text for details. Models used to generate the AOD lines include: GMI-MERRA-v3, GOCART-v4, LMDZ-INCA, OsloCTM2, and SPRINTARS-v385. Models used to generate the radiative forcing lines include all but the GMI-MERRA-v3 model. Model information and references can be found in Myhre et al. (2013).

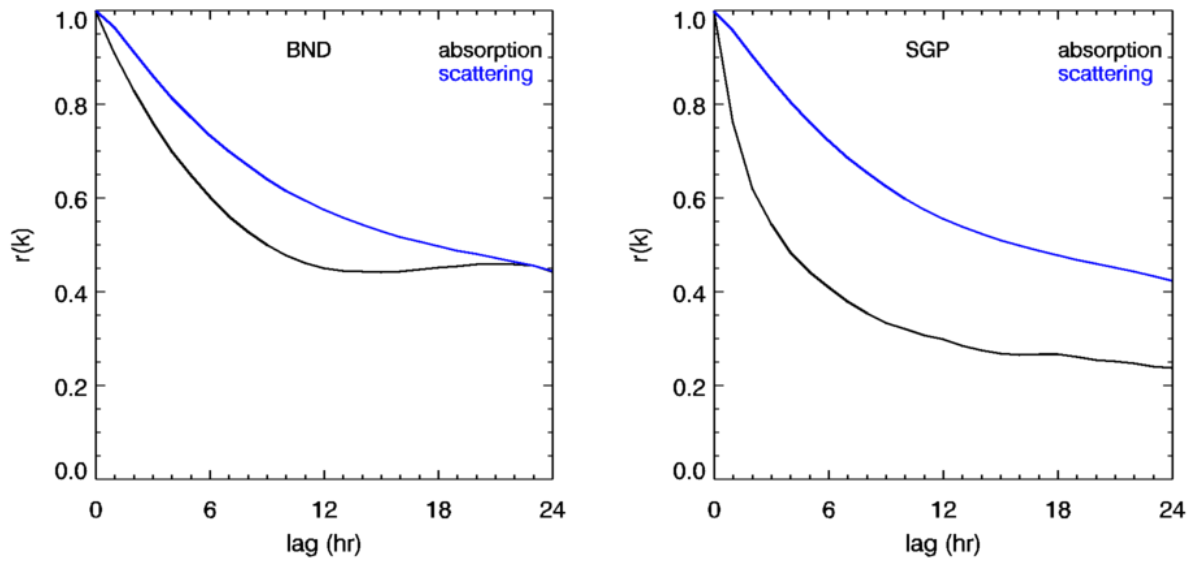


Figure 2. Correlograms for BND and SGP; wavelength = 550 nm, $D_p < 10 \mu\text{m}$, based on hourly averaged surface in-situ data between 1995-2013 (BND) and 1996-2013 (SGP). The value $r(k)$ on the y-axis represents the autocorrelation at lag time 'k'.

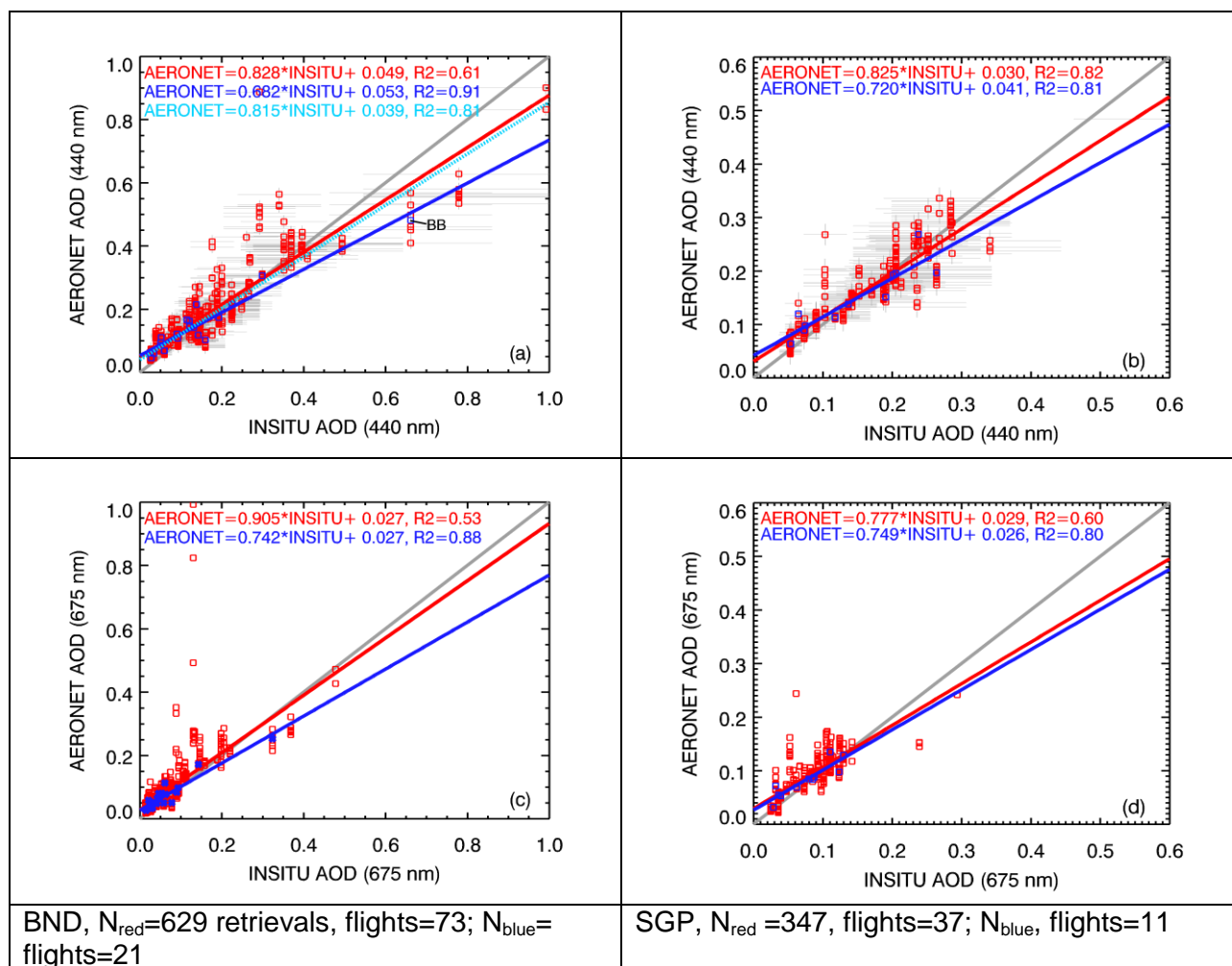


Figure 3. AOD comparison (a) BND at 440 nm; (b) SGP at 440 nm; (c) BND at 675 nm; and (d) SGP at 675 nm; thick gray line is 1 to 1 line. Thin gray lines associated with each data point represent measurement uncertainties. Red points and fit line represent all AERONET direct sun Level-2 AOD measurements within +/-3 hours of end of profile. Blue points and fit line represent the average of AERONET Level-2 AOD measurements with successful almucantar retrievals within +/-3 hours of end of profile. The light blue dashed line is the fit if the BB point is excluded. Note: two BND direct sun AOD440 points corresponding to the two highest AOD675 points in the figure below are off the scale of the plot and not shown. The third high AOD440 point is partly obscured by the legend.

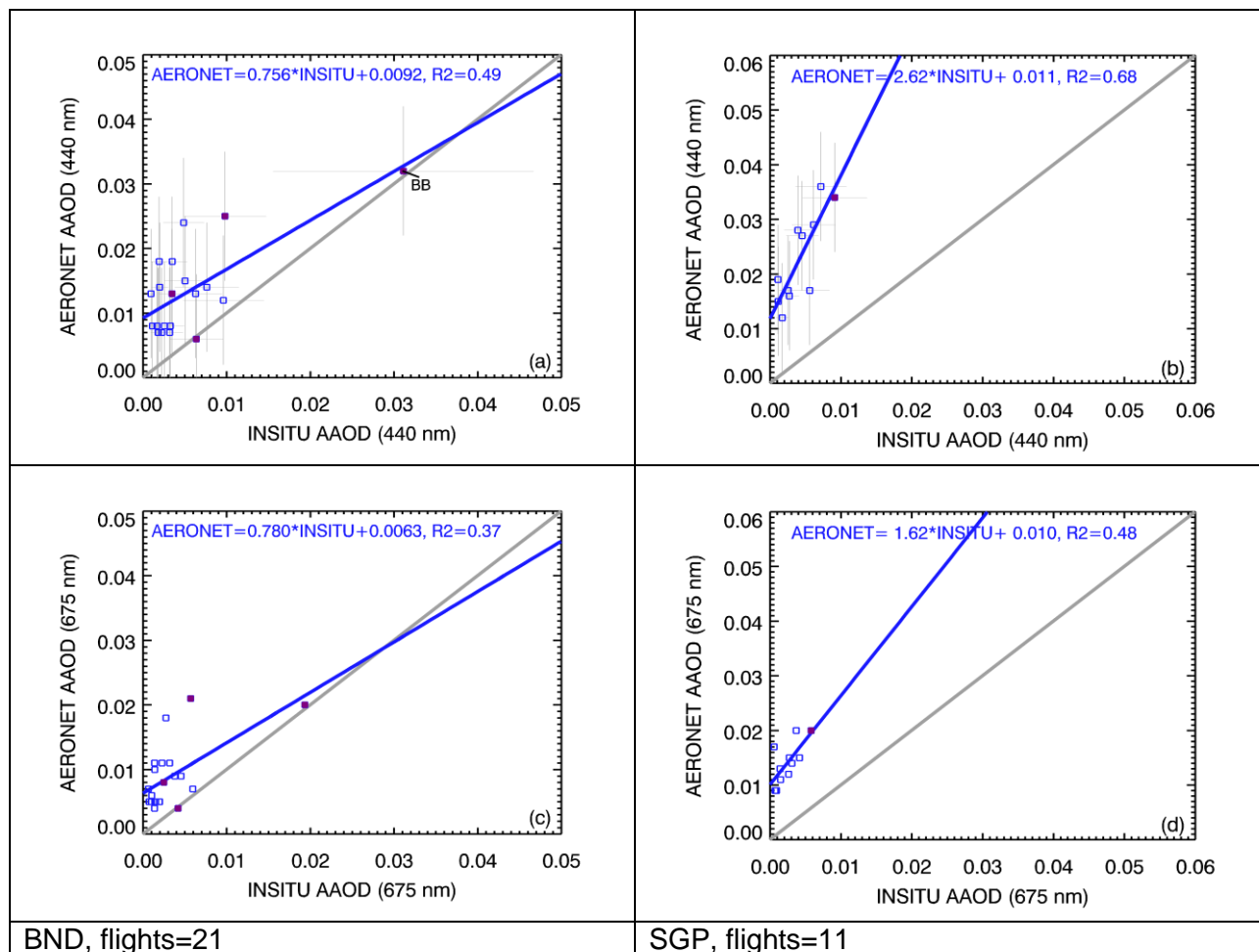


Figure 4. AAOD comparison, (a) BND at 440 nm; (b) SGP at 440 nm ; (c) BND at 675 nm; and (d) SGP at 675 nm. Blue line is linear fit for all points shown; gray line is 1 to 1 line. Thin gray lines associated with each data point represent measurement uncertainties. Points show the average of AERONET Level-1.5 AAOD retrievals for which there was a successful AERONET Level-2 almucantar retrieval within +/-3 hours of end of profile. Purple points indicate the few comparisons points for which there are AERONET Level-2 almucantar retrievals and where the average AERONET AOD₄₄₀ for those retrievals was great than 0.2.

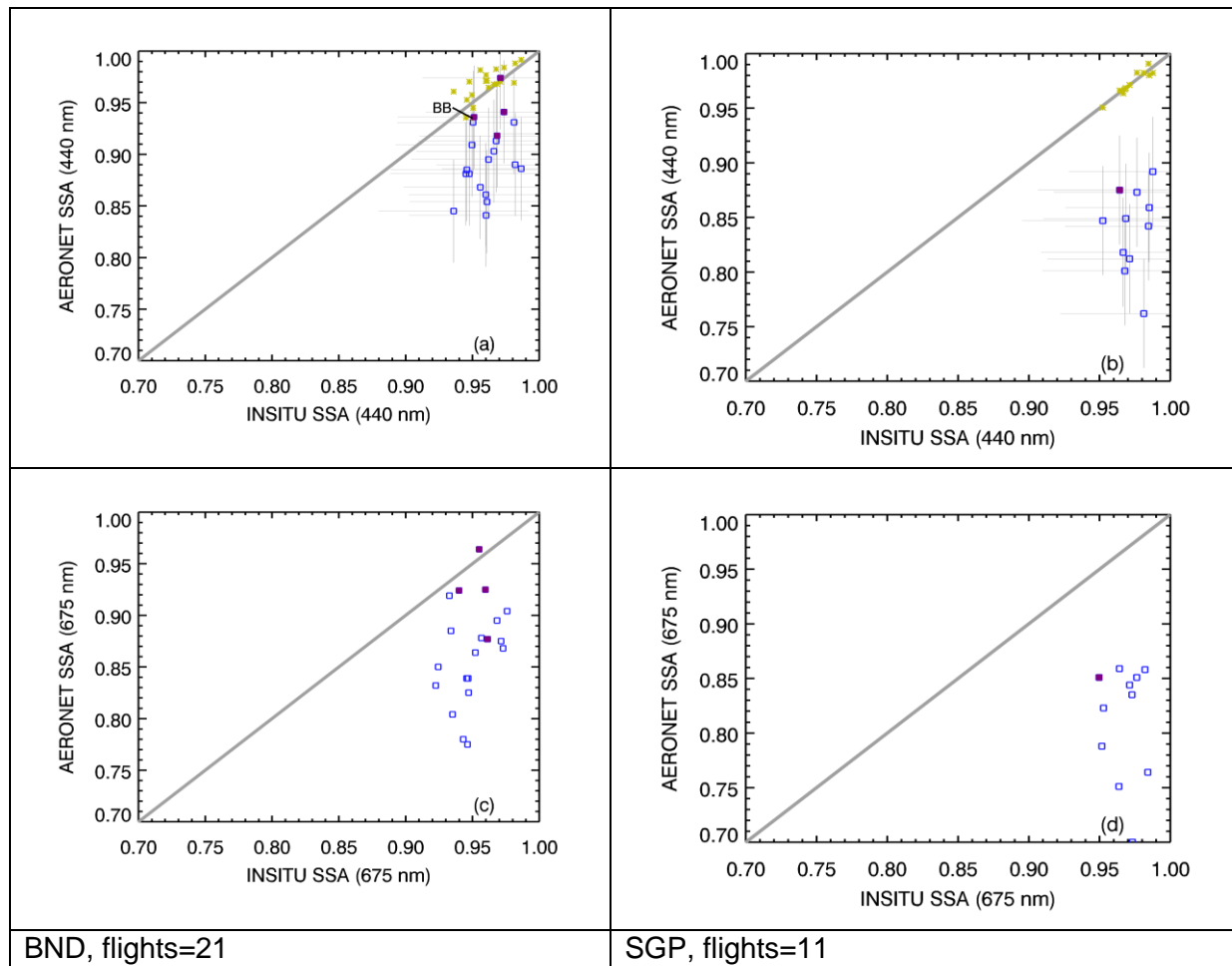


Figure 5. SSA comparison, (a) BND at 440 nm (b) SGP at 440 nm; (c) BND at 675 nm; and (d) SGP at 675 nm. Blue line is linear fit for all points shown; gray line is 1 to 1 line. Thin gray lines associated with each data point represent measurement uncertainties. Blue points show the average of all AERONET Level-1.5 AOD retrievals for which there was a successful AERONET Level-2 almucantar retrieval within +/-3 hours of end of profile. Purple points indicate the few points for which there are AERONET Level-2 almucantar retrievals and where the average AERONET AOD₄₄₀ for those retrievals was great than 0.2. The yellow points represent the 'hybrid SSA' which utilizes the AERONET AOD and the in-situ AOD to derive SSA as described in the text.

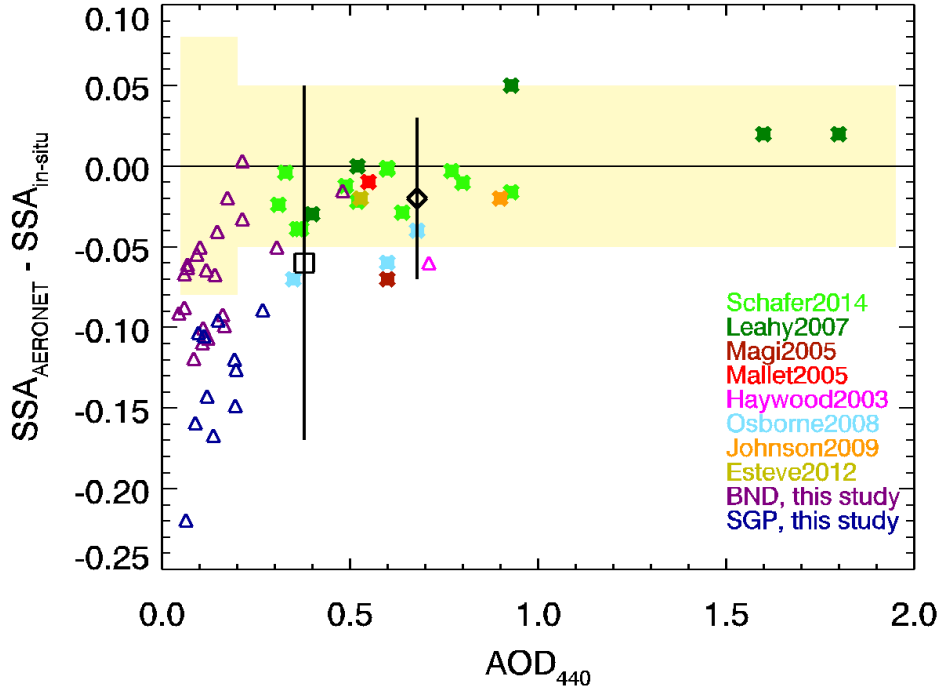


Figure 6. AOD_{440} vs $[SSA_{AERONET} - SSA_{INSITU}]$ for direct comparisons studies listed in Table 4. Open symbols are for SSA_{440} difference; filled symbols are for SSA_{550} difference. AOD_{440} values for Leahy2007, Osborne2008, Johnson2009 use the Level-2 values reported on the AERONET webpage for the locations and dates of the specific profile. Shading indicates combined uncertainty of AERONET SSA values as function of AOD as reported in Table 4 of Dubovik et al. (2000) and uncertainty in the in-situ SSA calculated using equation 2. The black square and black diamond with vertical black lines represent, respectively, the mean and 2*standard deviation for all direct comparisons (including BND and SGP) and for literature direct comparisons only.

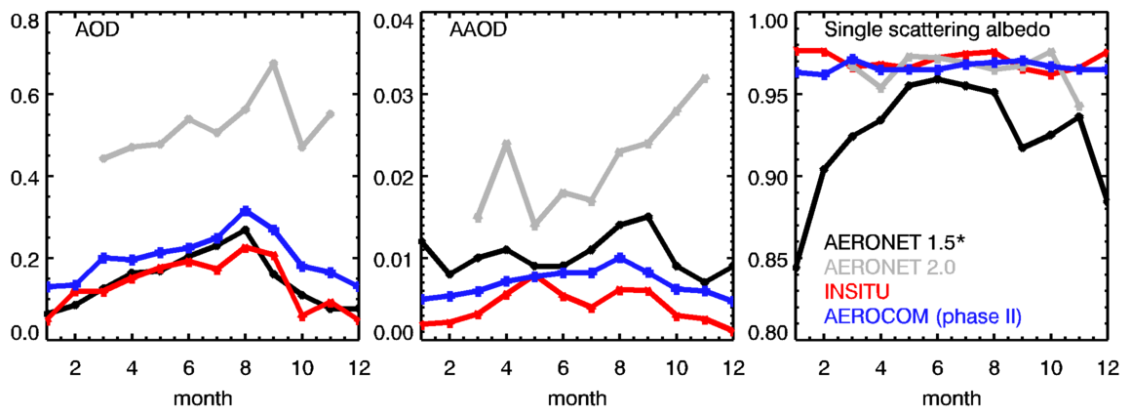


Figure 7a. Monthly medians of BND aerosol optical properties at 440 nm. AERONET medians are for 1996-2011. AERONET AOD medians are for observations with Level-2 almucantar retrievals, with corresponding AAOD and SSA retrievals at Level-1.5 (black) or Level-2 (gray). In-situ data are for June 2006-September 2009. AERONET Level-2.0 almucantar AOD and AAOD values are biased high by definition, because of the $AOD_{440} > 0.4$ constraint. AERONET 2.0 direct sun retrievals (not shown) are similar to the AERONET 1.5 AOD values. In-situ values are derived from 365 flights over BND. AeroCom Phase II median model results cover various time periods (depending on the model) and are reported at 550 nm.

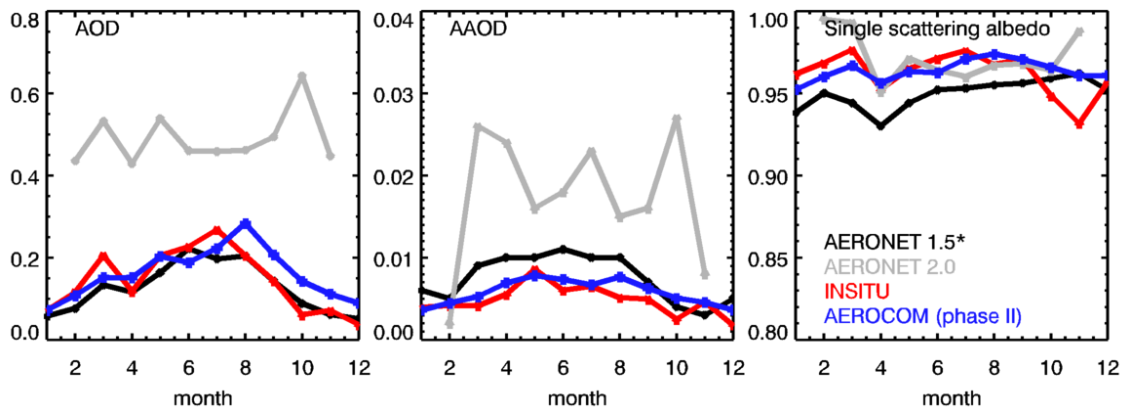


Figure 7b. Monthly medians of SGP aerosol optical properties at 440 nm. AERONET medians are for 1996-2011. In-situ data are for September 2005-December 2007. AERONET AOD medians are for observations with Level-2 almucantar retrievals, with corresponding AAOD and SSA retrievals at Level-1.5 (black) or Level-2 (gray). AERONET Level-2.0 almucantar AOD and AAOD values are biased high by definition, because of the $AOD_{440} > 0.4$ constraint. AERONET 2.0 direct sun retrievals (not shown) are similar to the AERONET 1.5 AOD values. In-situ values are derived from 322 flights over SGP. AeroCom Phase II median model results cover various time periods (depending on the model) and are reported at 550 nm.

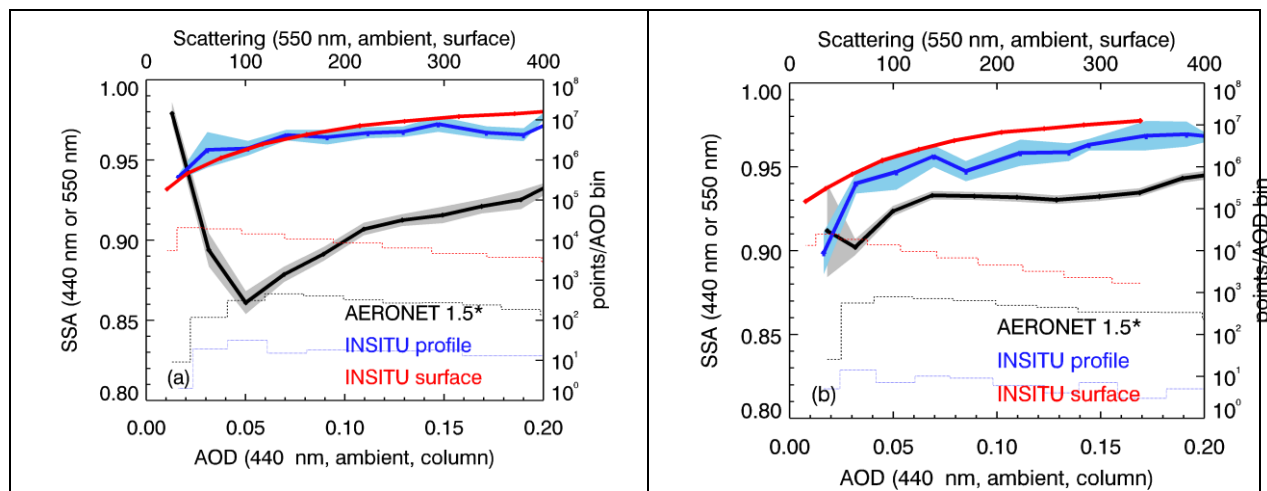


Figure 8. Systematic variability of SSA as a function of loading for (a) BND and (b) SGP for AERONET 1.5* AOD and SSA (black lines), AOD and SSA from in-situ profiles (blue lines) and in-situ scattering and SSA from surface measurements (red lines). Solid lines indicate mean values of SSA and AOD for each 0.05 AOD bin (10 Mm^{-1} scattering bin). Shaded areas represent mean standard error (mean standard error for surface data is within thickness of red line). Histograms indicate the number of points in each AOD (or scattering) bin. Plot based on BND and SGP AERONET data (date range: 1996-2012) and BND INSITU profile data (date range: 2006-2012); SGP INSITU profile data (date range: 2006-2007). Surface data (orange lines) are for 550 nm, low RH, hourly in-situ data from the surface sites at BND (date range: 1997-2013) and SGP (date range: 1998-2013). AERONET 1.5* is from Level-1.5 retrievals with a corresponding Level-2 almucantar retrieval.